iScience

CellPress
OPEN ACCESS

Article

EFNB1 levels determine distinct drug response patterns guiding precision therapy for B-cell neoplasms

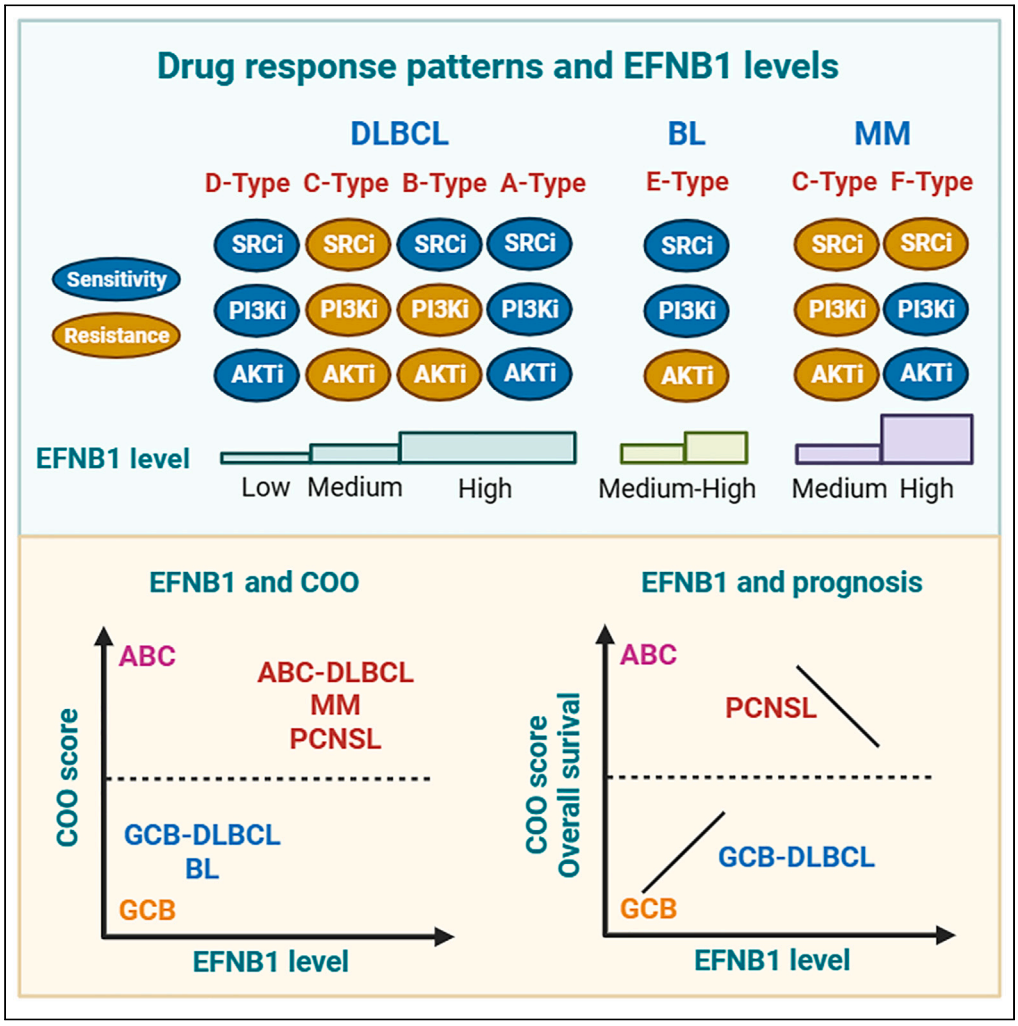

Xiaoxi Li, Chenxiao Zhang, Minyao Deng, Yong Jiang, Zhengjin He, Hui Qian

lixiaoxi@ujs.edu.cn (X.L.)
lstmmmlst@163.com (H.Q.)

Highlights

EFNB1 levels determine the response patterns of SRC-PI3K-AKT inhibitors

EFNB1 sensitizes cells to vincristine by promoting phosphorylation of STMN1

EFNB1 level is an indicator and the cause of B-cell lymphoma differentiation

EFNB1 is a potential biomarker for prognosis and drug efficacy prediction

Li et al., iScience 27, 108667
January 19, 2024
https://doi.org/10.1016/j.isci.2023.108667

iScience

CellPress
OPEN ACCESS

Article

EFNB1 levels determine distinct drug response patterns guiding precision therapy for B-cell neoplasms

Xiaoxi Li,[1,3,4,*] Chenxiao Zhang,[1,3] Minyao Deng,[1,3] Yong Jiang,[1] Zhengjin He,[2] and Hui Qian[1,*]

SUMMARY

The multi-omics data has greatly improved the molecular diagnosis of B-cell neoplasms, but there is still a lack of predictive biomarkers to guide precision therapy. Here, we analyzed publicly available data and found that B-cell neoplasm cell lines with different levels of EFNB1 had distinctive drug response patterns of inhibitors targeting SRC/PI3K/AKT. Overexpression of EFNB1 promoted phosphorylation of key proteins in drug response, such as SRC and STMN1, conferring sensitivity to SRC inhibitor and cytotoxic drugs. EFNB1 phosphorylation signaling network was significantly associated with the prognosis of GCB-DLBCL patients. Moreover, EFNB1 levels were correlated with cell of origin (COO) scores, suggesting that EFNB1 is a quantitative indicator of cell differentiation. Ultimately, we proposed a model for the stratification of human B-cell malignancies and the implementation of targeted therapies based on EFNB1 levels. Our findings highlight that EFNB1 level is a promising biomarker for predicting drug response, COO and prognosis.

INTRODUCTION

B-cell neoplasm is a highly heterogeneous lymphoid hyperplasia disease. Although R-CHOP (rituximab, cyclophosphamide, doxorubicin, vincristine and prednisone) regimen had achieved good therapeutic effect in diffuse large B-cell lymphoma (DLBCL), about 40% of patients still failed to benefit from the treatment.[1] Many factors can lead to treatment failure, such as extranodal dissemination. Extranodal dissemination is a typical feature of aggressive B-cell lymphoma, such as diffuse large B-cell lymphoma (DLBCL),[1] Burkitt's lymphoma (BL)[2] and high-grade B-cell lymphoma (HGBL).[3,4] On the one hand, extranodal dissemination is the result of the activation of pro-dissemination signals, which may directly lead to drug resistance. On the other hand, extranodal dissemination not only leads to the damage of involved tissues or organs, but also leads to insufficient drug concentration at disseminated sites. Therefore, extranodal dissemination is an important factor for treatment failure and a key prognostic indicator.

Based on gene expression profiles, the Cell of Origin (COO) classification divides DLBCL into 3 subtypes, activated B-cell (ABC) DLBCL, germinal center B-cell (GCB) DLBCL, and unclassified (UC) DLBCL.[5] The latest LymphGen classification further divides DLBCL into 7 subtypes based on the hallmarks of genetic variations.[6] Extranodal lymphoma mainly belongs to the MCD (MYD88-CD79) subtype.[6,7] The activating mutations causing chronic activation of the B cell receptor (BCR) signaling pathway, such as MYD88 L265P and CD79B mutations, promote the onset and progression of MCD-DLBCL. Ibrutinib and idelalisib, targeting BTK and PI3K respectively, are two approved targeted drugs used as a first-line treatment or to treat relapsed/refractory B-cell lymphoma.[8,9] Ibrutinib has substantial activity in the treatment of primary CNS lymphoma (PCNSL).[10,11] Ibrutinib plus R-CHOP have also been observed to enhance the survival benefit in MCD-DLBCL.[12] However, genetic and non-genetic resistance and adaptation to bypass the dependency on BCR inhibitors always develop through multiple mechanisms.[13] In addition, BCR signaling is also responsible for lymphocyte homing and adhesion via integrin.[14] Ibrutinib has been reported to promote the egress of malignant B cells from the lymph nodes into the peripheral blood in mantle cell lymphoma patients.[15] Therefore, inhibition of the BCR signaling pathway not only suppresses cell survival, but also promotes lymphoma dissemination. Hence, identifying genes involved in extranodal dissemination will be of great significance for understanding the pathogenesis of lymphoma and improving clinical efficacy.

EFNB1 (Ephrin B1) is a B-type ligand in the Eph-Ephrin family, which represents the largest superfamily of receptor tyrosine kinases (RTKs) and plays many functions in physiological and pathological processes.[16,17] The interaction of Eph receptors and Ephrin ligands on neighboring cells not only leads to the activation of the "forward" signal in Eph cells, but also phosphorylation of Ephrins and the activation of

[1]Department of Laboratory Medicine, School of Medicine, Jiangsu University, Zhenjiang, Jiangsu, China
[2]State Key Laboratory of Cell Biology, Shanghai Institute of Biochemistry and Cell Biology, Center for Excellence in Molecular Cell Science, Chinese Academy of Sciences, University of Chinese Academy of Sciences, Shanghai, China
[3]These authors contributed equally
[4]Lead contact
*Correspondence: lixiaoxi@ujs.edu.cn (X.L.), lstmmmlst@163.com (H.Q.)
https://doi.org/10.1016/j.isci.2023.108667

Table 1. The classification and genetic status of DLBCL cell lines

Cell lines	Lineage sub-subtype	COO classification[a]	MSI status	Mutational Burden	Ploidy WES	Gender
A3-KAW	DLBCL, NOS	ABC	MSS	56.5	2.12	Female
A4-FUK	DLBCL, NOS	ABC	MSS	37.76	2.16	Female
DB	DLBCL, NOS	GCB	MSS	32.42	3.25	Male
DOHH-2	DLBCL, NOS	GCB	MSS	24.26	2.06	Male
FARAGE	DLBCL, NOS	GCB	MSI	116.76	2.00	Female
HT	DLBCL, NOS	GCB	MSI	146.26	1.97	Male
KARPAS-422	DLBCL, NOS	GCB	MSS	40.97	2.16	Female
NU-DUL-1	DLBCL, NOS	ABC	MSS	30.16	2.00	Male
OCI-LY-19	DLBCL, NOS	GCB	MSS	21.05	2.07	Female
OCI-LY7	DLBCL, NOS	GCB	MSS	20.24	1.98	Male
RC-K8	DLBCL, NOS	UC[b]	MSS	53.42	2.12	Unknown
RL	DLBCL, NOS	GCB	MSS	39.87	2.09	Male
SU-DHL-10	DLBCL, NOS	GCB	MSS	22.21	2.05	Male
SU-DHL-4	DLBCL, NOS	GCB	MSS	28.74	2.18	Male
SU-DHL-5	DLBCL, NOS	GCB	MSS	32.71	1.98	Female
SU-DHL-6	DLBCL, NOS	GCB	MSS	36.21	2.10	Male
SU-DHL-8	DLBCL, NOS	ABC	MSS	39.13	2.25	Male
VAL	DLBCL, NOS	GCB	MSS	27.11	2.14	Female
WSU-DLCL2	DLBCL, NOS	GCB	MSS	27.55	2.06	Male

Abbreviation: COO, Cell of origin. DLBCL, NOS, Diffuse large B-cell lymphoma, not otherwise specified. MSI, microsatellite instability. MSS, microsatellite stability. WES, whole exon sequencing. UC, unclassified. ABC, activated B-cell. GCB, germinal center B-cell.

[a]COO classification is determined by RNA-seq-based COO score.

[b]RC-K8 cell line is identified as ABC-DLBCL in most literatures, GCB-DLBCL in DepMap database and UC by COO score.

the "reverse" signal in Ephrin cells. The Ephs and Ephrins can also trigger signals independently through interplay with other signal components.[18–20] The expression level of Ephs and Ephrins is critical for their clustering and biological functions. EFNB1 has been reported as a specific marker for mature germinal center (GC) B cells[21] and can control the function of germinal center T cell with EPHB4 and EPHB6.[22] Moreover, EFNB1 has been reported to contribute to tumor progression in many cancers.[17,23] Our previous study revealed that Efnb1 can promote extranodal dissemination of lymphoma in Eμ-Myc; Utx^{KO} mouse model and high expression of Efnb1 is significantly associated with poor prognosis of human DLBCL.[24] Given the potential effect of BCR activation on extranodal dissemination, we guess that EFNB1 may have a crosstalk with the BCR signaling pathway, thereby modulating therapeutic response of BCR-associated kinase inhibitors. In this study, we analyzed the correlation of EFNB1 level and drug response pattern in human DLBCL, BL, and Multiple Myeloma (MM) cell lines and identified six distinct drug response patterns of SRC/PI3K/AKT inhibitors. Moreover, EFNB1 levels were significantly associated with cell of origin. These results indicate that EFNB1 level is a promising biomarker for predicting drug response, COO and prognosis.

RESULTS

EFNB1 levels are associated with drug response patterns of SRC-PI3K-AKT inhibitors in the DLBCL cell lines

Abnormal activation of the BCR signaling pathway is a typical feature of MCD-DLBCL, and inhibitors of BCR-associated kinases have become a new choice of the treatment of B-cell malignancies. To explore the role of EFNB1 on drug response, we selected 19 DLBCL cell lines (Table 1) with available IC50 data (half-maximal inhibitory concentration) and analyzed their EFNB1 expression level. Eleven BCR-associated kinase inhibitors, targeting ABL-SRC/ABL/SYK/BTK/PI3K/AKT, were selected as the BCR inhibitors panel (Figure 1A).

Based on the overall drug response and EFNB1 level, 19 DLBCL cell lines could be divided into two groups. The low-EFNB1 group was sensitive to targeted drugs, while the high-EFNB1 group was tolerant to targeted drugs. According to the drug response patterns of ABL-SRC/PI3K/AKT, we further divided the high-EFNB1 cell lines into 3 groups. In total, according to the drug response patterns and EFNB1 levels, 19 DLBCL cell lines were stratified into four drug response patterns and three EFNB1 levels: A/B/C/D-Types and high/medium/low levels (Figure 1B). Based on the difference in response to PI3K-AKT inhibitors, $EFNB1^{high}$ cell lines (TPM>=1.94) were divided into two types, sensitive A-Type and resistant B-Type. $EFNB1^{medium}$ cell lines (1.37<=TPM<=1.79), classified as C-Type, were resistant to all targeted drugs. $EFNB1^{low}$ cell lines (TPM<=1.24), classified as D-Type, were sensitive to most targeted drugs rather than ABL-BTK-SYK inhibitors. It should be noting that the correlation between some cell lines and certain drugs is not completely consistent with the A/B/C/D-type drug response pattern, such as HT and RL, indicating the existence of alternative mechanisms in addition to EFNB1 levels. For instance, the HT cell line is MSI (microsatellite instability), which may contribute to its unexpected drug response pattern. Therefore, HT and RL were classified as "Others".

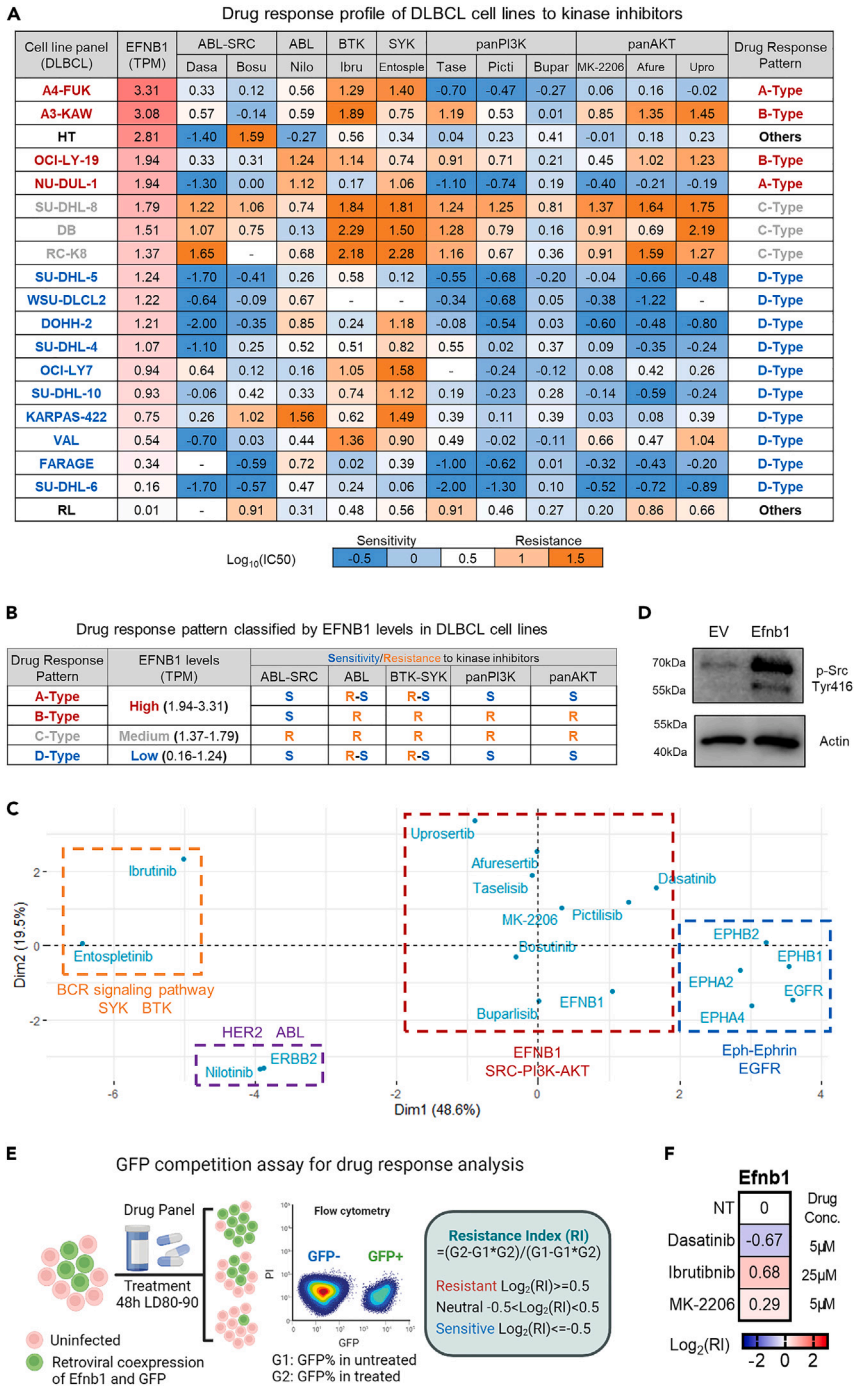

Figure 1. EFNB1 levels are associated with drug response patterns of SRC-PI3K-AKT inhibitors in DLBCL cell lines

See also Figure S1.

(A) Drug response profile of targeted drugs in DLBCL cell line. Efnb1 levels were evaluated by TPM. TPM, Transcripts Per Kilobase per Million mapped reads. Drug response was evaluated by IC50, the half maximal inhibitory concentration. The unit for IC50 is μM. Dasa, Dasatinib. Bosu, Bosutinib. Nilo, Nilotinib. Ibru, Ibrutinib. Entosple, Entospletinib. Tase, Taselisib. Picti, Pictilisib. Bupar, Buparlisib. Afure, Afuresertib. Upro, Uprosertib.

(B) Four drug response patterns in three EFNB1-Level groups of DLBCL cell lines. 19 DLBCL cell lines were divided into three EFNB1-level groups and four drug response patterns. The EFNB1^{high} group was further divided into A-Type and B-Type patterns, the EFNB1^{medium} group was C-Type pattern, and the EFNB1^{low} group was D-Type pattern.

(C) Western bolt analysis of the phosphorylation level of SRC at 416 tyrosine. EV, empty vector.

Figure 1. *Continued*

(D) Correspondence analysis of the expression pattern of EFNB1-related genes and the IC50 pattern of SRC-PI3K-AKT. The principal component analysis was performed based on the expression level of EFNB1 (TPM) and IC50 of kinase inhibitors in 19 DLBCL cell lines. Red dotted box, EFNB1 levels and BCR SRC-PI3K-AKT inhibitors. Yellow dotted box, SYK-BTK inhibitors. Blue dotted box, Eph receptors levels and EGFR levels. Purple dotted box, ABL inhibitor and HER2 levels.

(E) Diagram of GFP competition assay. Retroviral Efnb1 and GFP co-expressed cells were mixed with uninfected cells for drug treatment. The drug concentration was determined according to the lethal dose of drug treatment for 48h, usually reaching LD80-90. LD, Lethal dosage, evaluated by cell viability (PI-%). PI, propidium iodide. The GFP ratio of untreated cells and treated cells was analyzed at 72h. G1 represented the GFP ratio of untreated cells, and G2 represented the GFP ratio of drug treated cells. Calculate the Resistance Index (RI), RI = (G2-G1 *G2)/(G1-G1 *G2), and evaluate the effect of genes on drug response.

(F) GFP competition assay of EFNB1 on targeted drugs. Log2 (RI) $\geq$0.5 was considered as resistance; Log2 (RI) $\leq$-0.5 was considered as sensitivity; otherwise, it was neutral. NT, untreated.

Most targeted drugs inhibit tumor growth by suppressing pro-survival or pro-proliferation signaling. If some cell lines are more sensitive to targeted drugs, it indicates that their survival depends more on the related signaling pathways. D-Type pattern showed that the EFNB1^{low} cell lines are sensitive to most ABL-SRC/PI3K/AKT inhibitors, indicating that the PI3K-AKT signaling pathway is the key pro-survival pathway, thereby it can be recognized as the vulnerability for the EFNB1^{low} cell lines. The C-type pattern showed that most of the tested inhibitors are unable to inhibit proliferation of the EFNB1^{medium} cell lines, suggesting the presence of additional proliferative signals. Moreover, A-Type EFNB1^{high} cell lines are highly dependent on the PI3K-AKT pathway, but B-Type EFNB1^{high} cell lines are not. In addition, we noticed that the EFNB1^{high} cell lines are sensitive to multi-kinase inhibitor, such as Dasatinib targeting ABL and SRC, and resistant to ABL inhibitors, such as Nilotinib. Hence, we guessed that the EFNB1^{high} cell lines are highly dependent on the SRC-related pathway rather than ABL-related pathway.

To verify the specificity of EFNB1 levels and drug response patterns, we performed the correspondence analysis between the expression level of EFNB1 and several other RTK genes and the IC50 values of targeted drugs in the DLBCL cell lines. Two B-type Eph receptors, EPHB1 and EPHB2, were well-established receptors for EFNB1, and two A-type Eph receptors, EPHA2 and EPHA4, were newly identified as receptors for EFNB1 in immune cells.[25] Therefore, we finally analyzed the four EFNB1 receptors, EPHB1, EPHB2, EPHA2, EPHA4 and the other two RTKs, EGFR, and HER2. Principal component analysis showed that the expression pattern of EFNB1 in the DLBCL cell lines was clustered together with the IC50 pattern of SRC-PI3K-AKT inhibitors (Figure 1C). In addition, the four EFNB1's receptors and EGFR are clustered together. The HER2 level is closely clustered with the IC50 pattern of the ABL inhibitor, Nilotinib. The IC50 patterns of Ibrutinib and Entospletinib, targeting two key BCR inhibitors BTK and SYK respectively, have the lowest correlation with others. Together, these results suggested that the correlation between EFNB1 levels and drug response patterns is specific.

To verify the observation from human DLBCL cell lines, we performed the experimental verification on *Eμ-Myc;Cdkn2a−/−* cell line. *Eμ-Myc;Cdkn2a−/−* cell line is a murine lymphoma derived cell line with well-defined genetic background and widely used in drug response analysis.[26,27] As SRC is an interacting protein of Efnb1[28] and can be phosphorylated by EphB/Ephrin B,[29] we established an EFNB1-overexpressed stable cell line and analyzed the phosphorylation level of SRC. The results showed that ectopic expression of Efnb1 significantly enhanced phosphorylation of SRC at tyrosine 416 (Figure 1D). To verify the interaction of EFNB1 and kinase inhibitors, we performed GFP competition assay in the *Eμ-Myc;Cdkn2a*$^{-/-}$ cell line (Figure 1E). GFP competition assay was designed to determine the survival advantage of genetically modified cells under drug-induced selection pressure. The results showed that overexpression of Efnb1 conferred cells sensitive to dasatinib and resistant to Ibrutinib (Figure 1F), which was consistent with B-Type pattern in the EFNB1^{high} cell lines. Together, these results suggested that the activation of the EFNB1-SRC axis can enhance the cell dependency on SRC-related pathway, and thereby increase the sensitivity of EFNB1^{high} cells to SRC inhibitors.

To further explore the signaling pathways related to targeted drug response, we analyzed the publicly available protein expression dataset of DLBCL cell lines, which was generated by reverse-phase protein arrays (RPPAs).[30] RPPA is a quantitative, antibody-based technology, in which cell or tissue proteins will be printed on nitrocellulose-coated slides and analyzed by a set of antibody probes. 214 proteins and phosphoproteins covering major cancer signaling pathways are available in the dataset of DLBCL cell lines. Based on the observed differences in drug response, we analyzed differentially expressed proteins/phosphoproteins (DEPs/DEPPs) in different drug response patterns and the merged patterns as indicated comparisons (See Figure S1A; Table S1). Phosphorylated AKT is one of five DEPs/DEPPs between A-Type and B-Type cell lines (See Figure S1B), which is consistent with their difference in drug response to PI3K-AKT inhibitors. Many DEPs/DEPPs were identified in A&B-Type vs. D-Type comparison and C-Type vs. D-Type comparison, involving the PI3K-AKT-mTOR and RAF-MEK1-JUN signaling pathways (See Figure S1B), indicating that D-Type cell lines are significantly different from A/B/C types in terms of the signaling network, supporting their overall differences in drug response pattern. Together, these results suggested that the level and activity of kinase proteins are key reasons for the differences in drug response and cell dependency.

We also analyzed the correlation of EFNB1 level and the phosphorylation status of SRC in RPPA data. We found that some EFNB1^{high} cell lines had increased SRC phosphorylation, such as HT (Src_pY416), A3KAW (Src_pY527), while some EFNB1^{low} cell lines had lower SRC phosphorylation, such as KARPAS422 (Src_pY416), SUDHL6 (Src_pY527) (See Figures S1C–S1E). However, there was a lack of statistical correlation between EFNB1 level and SRC phosphorylation in all DLBCL cell lines. The lack of correlation between SRC phosphorylation levels and EFNB1 level may be attributed to the heterogeneous genetic backgrounds of the cell lines and their complex signaling network. We will discuss in detail the possible reasons in the discussion section.

In summary, we identified four drug response patterns and three EFNB1-level groups based on the expression level of EFNB1 in DLBCL cell lines and their IC50s to BCR-associated kinase inhibitors. Ectopic expression of EFNB1 can promote SRC phosphorylation and confer cells sensitivity to SRC inhibitors. These results suggest that EFNB1 can interfere with the pro-proliferation signals and cell dependency on BCR-associated kinases.

EFNB1 confers chemo-susceptibility

Changes in intrinsic signaling pathways and networks may alter the expression of genes related to cytotoxic drug response, thereby indirectly affecting the sensitivity of cells to cytotoxic drugs. To investigate the effect of EFNB1 on chemotherapy, we analyzed the drug response pattern of EFNB1 on lymphoma cytotoxic drug panel. Cytarabine (Ara-C) and Methotrexate (MTX) in R-HyperCVAD, Doxorubicin (DOX) and Vincristine (VCR) in R-CHOP regimen, Gemcitabine (GEM) in R-GCVP regimen, Etoposide (VP-16) in R-CEPP regimen, Cisplatin (CDDP) in R-ICE regimen, Oxaliplatin (OXA) in DHAX regimen, and VNB in GemVNB regimen were selected.

Firstly, we analyzed the EFNB1 level and the IC50 of cytotoxic drugs in human DLBCL cell lines. There was a poor correlation between the EFNB1 level and the IC50 of cytotoxic drugs, but there was indeed a difference in the number of cell lines sensitive to drugs in EFNB1$^{high\text{-}medium}$ and EFNB1^{low} cell lines (Figure 2A). The number of EFNB1 $^{high\text{-}medium}$ cell lines sensitive to Ara-C, MTX, CDDP was a little higher than that of EFNB1^{low} cell lines (Figure 2B). Overall, the DLBCL cell lines display intrinsic sensitivity to a variety of cytotoxic drugs, which may be determined by the characteristics of the DLBCL cells themselves, such as suspension. In the GDSC database, most sensitive cell lines are suspended cell lines, such as leukemia, lymphoma, multiple myeloma cell lines. Suspended tumor cells often are 50–1000 times more sensitive to cytotoxic drugs than adherent tumor cells.

Next, GFP competition assay was performed to verify the effect of EFNB1 on cytotoxic drugs. Surprisingly, Efnb1-overexpressed cells were hypersensitive to most cytotoxic drugs, especially DOX and VCR in R-CHOP regimen (Figure 2C). The gradient dose assay further verified the gene-drug interaction of Efnb1-DOX (Figure 2D) and Efnb1-VCR (Figure 2E). The IC50 of DOX for EV cells was 140 nM and the IC50 of DOX for EFNB1 cells was 68.8 nM. Due to the narrow range of VCR lethal dose (5–10 nM), we could not calculate the IC50 data. Bar graph presentation showed that EFNB1 cells were almost dead at 5 nM VCR, while EV cells were alive at 5 and 7.5 nM. In addition, Decitabine (DAC), an inhibitor of DNA methyltransferase (DNMTi), was analyzed as a negative control (Figure 2F). These results indicate that ectopic expression of EFNB1 can significantly enhance the sensitivity of cells to most cytotoxic drugs.

Together, these results indicate that ectopic expression of Efnb1 significantly enhances the sensitivity of cells to most cytotoxic drugs. EFNB1 agonists may act as chemosensitizers, combining with chemotherapy drugs to improve the efficacy and reduce the toxicity.

EFNB1 phosphorylation signaling network contributes to chemo-susceptibility

To explore the mechanism, we analyzed proteins and phosphorylated peptides in EV and Efnb1 cells by mass spectrometry. Totally, 35994 peptides, involving 4135 proteins, were identified in EV and Efnb1 cells. After being filtered with the indicated parameters, 96 unique differential proteins (DPs), 91 differentially expressed proteins (DEPs), and 161 phosphorylated peptides were identified (Figure 3A). Pathway enrichment analysis showed that EFNB1 significantly affected cell cycle and DNA repair signaling pathways (Figure 3B). These results suggest that abnormalities in cell cycle and DNA repair caused by Efnb1 may contribute to chemo-susceptibility.

In 161 phosphorylated peptides, 50 phosphorylated peptides, involving 41 proteins, were identified in EFNB1 cells (Figure 3C, See Table S2) and recognized as the members of the EFNB1 phosphorylation signaling network. Among them, TOP2A is a previously reported gene associated with the sensitivity of topoisomerase inhibitors.[31] STMN1 is a microtubule-associated protein, and its phosphorylation regulation plays a key role in the cell cycle.[32] Many studies report that the expression level of STMN1 is associated with chemoresistance of vinca alkaloids and taxanes.[33,34]

To investigate whether the phosphorylation of STMN1 at Serine 28 can affect the response of cells to VCR, we constructed the wild-type Stmn1 and S28A mutant cell lines. GFP competition analysis showed that ectopic expression of the wild-type Stmn1 greatly sensitized cells to VCR (Figures 3D–3G), while the S28A mutant conferred weaker sensitivity of cells to VCR (Figures 3H and 3I). The result indicates that increased phosphorylation of STMN1 at Serine 28 contributes to the Efnb1-conferred sensitivity to VCR.

Together, these results support that EFNB1 phosphorylation signaling network contributed to chemo-susceptibility of EFNB1^{high} cells.

The EFNB1 phosphorylation signaling network is associated with the prognosis of GCB-DLBCL

To investigate the clinical relevance of the EFNB1 phosphorylation signaling network in DLBCL patients, we performed survival analysis for all 41 genes, corresponding to 41 phosphorylated proteins identified in Efnb1 cells (Figure 3C, See Table S2). The result showed that high expression of seven genes (MCM2, ATXN2L, HDLBP, NPM1, PA2G4, TRMT61A, UBAP2L) was significantly associated with poor prognosis of DLBCL patients (Lenz-Staudt, DLBCL, GSE10846) (Figures 4A and 4B). Next, we analyzed whether the joint expression of EFNB1 and the seven genes has a better predictive effect. Among them, only the joint expression of EFNB1 and MCM2 presented a better effect on the prognostic prediction in DLBCL (Figure 4C).

Furthermore, we asked whether the EFNB1 phosphorylation signaling network is associated with DLBCL subtypes. We performed the survival analysis for EFNB1 and the seven genes in ABC, GCB, and UC subtypes (Figures 4D–4F). The results showed that all genes except TRMT61A were significantly associated with the prognosis of GCB subtype (Figure 4E), suggesting that the EFNB1 phosphorylation signaling network contributes to the malignant progression of GCB-DLBCL. Next, we performed the survival analysis on patients with three subtypes of DLBCL using the joint expression level of the eight genes. The results showed that the joint expression level of the eight genes could

A

Drug response profile of DLBCL cell lines to cytotoxic drugs

Cell line panel (DLBCL)	EFNB1	Antimetabolites			Topo inhibitors		DNA crosslinker		Mitosis	
	(TPM)	Ara-C	MTX	GEM	DOX	VP-16	CDDP	OXA	VCR	VNB
A4-FUK	3.31	0.0	-	-1.7	-0.5	0.0	0.9	0.9	-2.2	-2.6
A3-KAW	3.08	0.1	-1.7	-2.2	-1.1	-0.4	0.7	0.1	-1.7	-2.5
HT*	2.81	0.9	1.3	-1.3	-0.4	1.2	1.6	1.6	-	-2.4
OCI-LY-19	1.94	-1.2	0.7	-2.6	-1.1	-0.9	0.5	0.7	-	-2.5
NU-DUL-1	1.94	-1.7	0.9	-2.7	-0.2	-0.2	0.4	0.1	-	-2.6
SU-DHL-8	1.79	-	-1.4	-1.6	-0.7	-0.5	1.3	0.3	-1.4	-1.3
DB	1.51	-0.5	-1.3	-2.1	-1.0	0.8	0.7	0.5	-2.1	-2.1
RC-K8	1.37	1.2	-	-1.3	0.2	1.0	1.6	0.6	-1.4	-0.8
SU-DHL-5	1.24	-0.8	-1.7	-2.4	-2.3	-1.2	-	1.2	-2.9	-2.5
WSU-DLCL2	1.22	0.3	-	-2.5	-0.1	2.1	1.6	0.8	-	-2.7
DOHH-2	1.21	0.0	0.5	-1.9	-	-0.5	0.6	0.6	-2.6	-2.6
SU-DHL-4	1.07	0.8	0.9	-2.2	-0.5	1.2	1.2	1.2	-	-2.4
OCI-LY7	0.94	0.4	-1.1	-2.6	-0.3	-	1.2	0.8	-	-2.6
SU-DHL-10	0.93	-	-1.6	-2.0	-0.6	-0.5	1.5	0.9	-2.3	-2.5
KARPAS-422	0.75	0.7	-0.2	-0.6	-0.6	0.7	1.4	1.0	-1.7	-1.6
VAL	0.54	-1.0	0.9	-2.1	-0.2	1.1	1.4	0.5	-1.5	-2.1
FARAGE	0.34	0.9	0.3	-2.6	0.6	-0.7	1.5	0.2	-2.3	-3.0
SU-DHL-6	0.16	-0.2	-	-1.3	-0.3	0.2	-	0.8	-2.2	-2.8
RL*	0.01	0.2	0.7	-2.2	-1.4	2.2	1.5	0.8	-	-2.9

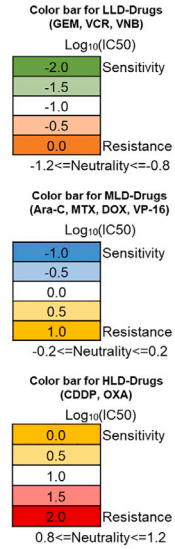

B

Drug response pattern of chemotherapy drugs based on EFNB1 level

Drugs	Ara-C		MTX		GEM		DOX		VP-16		CDDP		OXA		VCR		VNB	
Drug Response	S	R	S	R	S	R	S	R	S	R	S	R	S	R	S	R	S	R
EFNB1^{high} EFNB1^{medium}	3	1	3	2	7	0	6	0	3	3	4	2	6	0	5	0	6	0
	50%	17%	60%	40%	100%	0%	71%	0%	43%	29%	57%	29%	86%	0%	100%	0%	86%	0%
EFNB1^{low}	2	5	3	4	9	1	6	1	4	4	1	5	3	0	7	0	10	0
	22%	50%	38%	50%	90%	10%	67%	11%	44%	44%	13%	63%	30%	0%	100%	0%	100%	0%

C

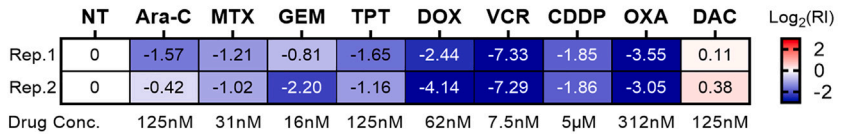

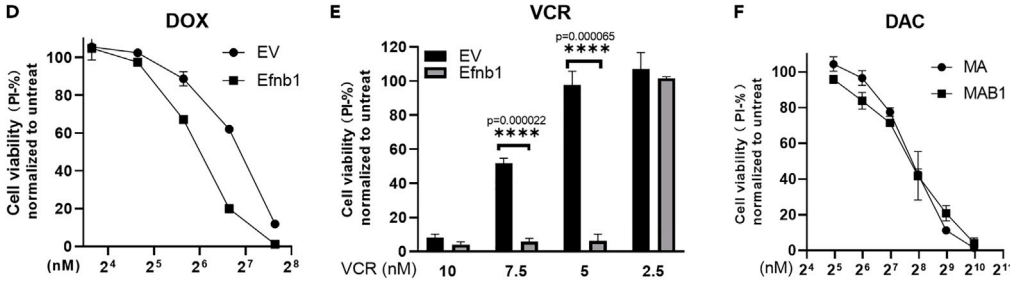

Figure 2. Ectopic expression of EFNB1 confers cells sensitivity to most cytotoxic drugs

(A) Drug response profile of cytotoxic drugs in DLBCL cell line. Ara-C, Cytarabine. MTX, Methotrexate. GEM, Gemcitabine. DOX, Doxorubicin. VP-16, Etoposide. CDDP, Cisplatin. OXA, Oxaliplatin. VCR, Vincristine. VNB, Vinorelbine. The logarithm of IC50 data was taken and drugs with different lethal doses were evaluated separately. A lethal dose of around 0.1μM was defined as low lethal dose (LLD). A lethal dose of around 1μM was defined as medium lethal dose (MLD). A lethal dose of around 10μM was defined as high lethal dose (HLD). "-" indicated that the IC50 data was unavailable. Color bars for LLD/MLD/HLD indicate the range of Log_{10}(IC50) for each drug.

(B) The number and relative proportion of sensitive or resistant cell lines in EFNB1 $^{high\text{-}medium}$ cell lines and EFNB1^{low} cell lines.

(C) GFP competition assay of EFNB1 on the lymphoma drug panel. Ara-C, Cytarabine. MTX, Methotrexate. GEM, Gemcitabine. TPT, Topotecan. DOX, Doxorubicin. VCR, Vincristine. CDDP, Cisplatin. OXA, Oxaliplatin. DAC, Decitabine. Log2 (RI) ≥0.5 was considered as resistance; Log2 (RI)≤-0.5 was considered as sensitivity; otherwise, it was neutral. NT, untreated.

(D) Gradient dose analysis of DOX on EV and Efnb1. Cell viability was measured by PI-% at 48 h post treatment. $IC50_{DOX}$(EV) = 140nM, $IC50_{DOX}$(Efnb1) = 68.6nM.

(E) Gradient dose analysis of VCR on EV and Efnb1. Cell viability was measured by PI-% at 48 h post treatment. Unpaired t-test was used to test the significance.

(F) Gradient dose analysis of DAC on EV and Efnb1. Cell viability was measured by PI-% at 48 h post treatment. Data are obtained from three technical replicates. Data are presented as mean ± SEM. *p < 0.05, **p < 0.01, ***p < 0.001, ****p < 0.0001 and n.s. indicates not significant (p > 0.05).

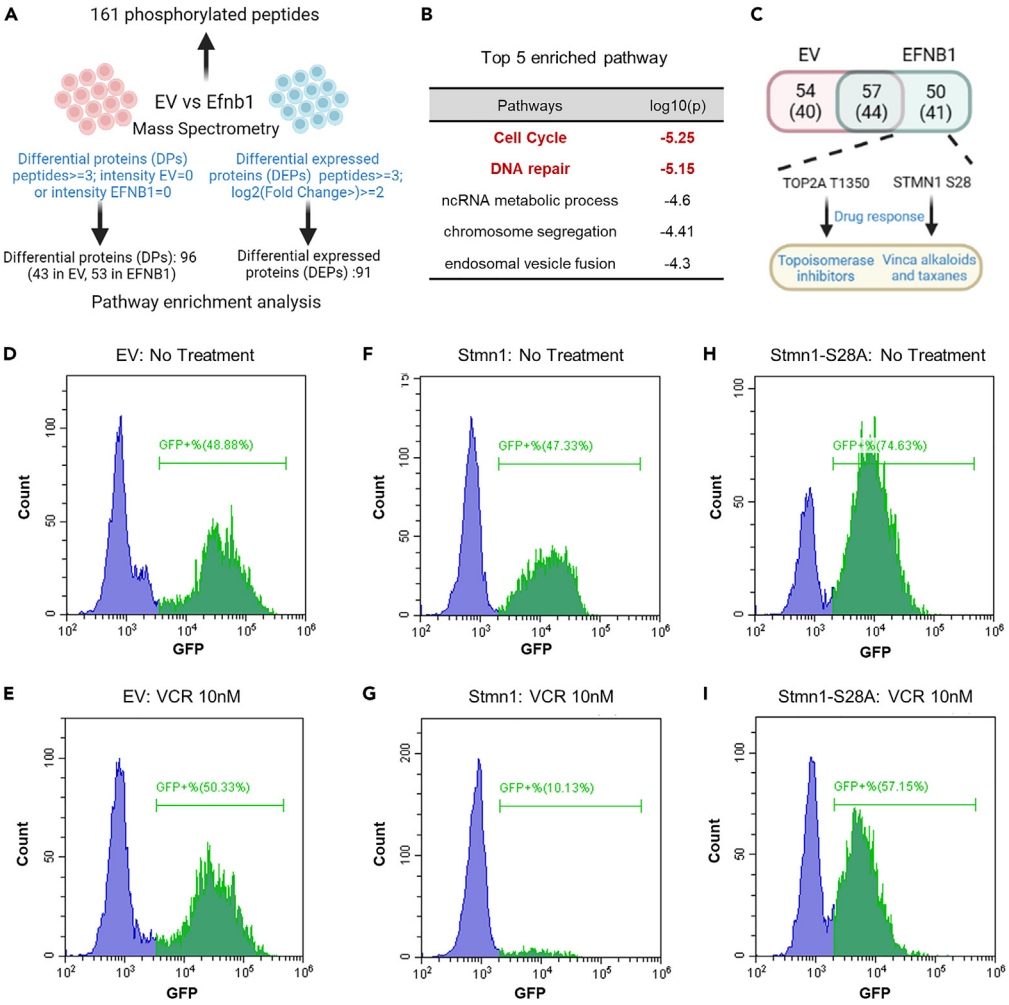

Figure 3. EFNB1 phosphorylation signaling network is associated with drug sensitivity

See also Table S2.

(A) Mass spectrometry data analysis scheme of EV and Efnb11 cells. EV, empty vector. Differential proteins (DPs) refer to proteins only detected in EV or Efnb1, and the peptides ≥ 3. Differently expressed proteins (DEPs) refer to proteins that were detected in both, and the peptides ≥ 3, the relative intensity was more than 4-fold. 96 DPs, 91 DEPs, and 161 phosphorylation sites/peptides (125 proteins) were identified.

(B) Top 5 pathways enriched in DPs and DEPs.

(C) Distribution of 161 phosphorylation sites/peptides (125 proteins) in EV and Efnb1. (D-E). EV-GFP cell population without treatment (D) and with VCR (E).

(F and G) Stmn1-GFP cell population without treatment (F) and with VCR (G).

(H–I) Stmn1-S28A-GFP cell population without treatment (H) and with VCR (I).

effectively distinguish high-risk and low-risk populations in both DLBCL (Figure 4G) and three subtypes of DLBCL (Figures 4H–4J), suggesting that the 8-gene signature is a potential prognostic biomarker for DLBCL. Together, these results suggest that the EFNB1 phosphorylation signaling network is closely related to the prognosis of DLBCL patients, indicating that it is more likely to affect the treatment response of DLBCL.

EFNB1 level is an indicator and cause of B-cell lymphoma differentiation

Cell of origin, as one of the pathological mechanisms, is an important indicator for the classification and prognosis of B-cell malignancies. To investigate the effect of EFNB1 on the cell of origin, we used an RNA-seq based method[35,36] to calculate the COO score of the DLBCL cell lines. The COO score is calculated from the expression levels of 20 genes associated with ABC/GCB classification, and can be used to determine the ABC/GCB origin of lymphoma.

The results showed a significant correlation between EFNB1 levels and COO scores ($p = 0.0070$, **) in the DLBCL cell lines (Figure 5A, See Table S3). The EFNB1 level in ABC cell lines was significantly higher than that in GCB cell lines ($p = 0.0058$ **) (Figure 5B). Next, we analyzed the relevance between EFNB1 level, COO score and drug response pattern. ABC cell lines are mainly EFNB1$^{medium\text{-}high}$ cells (TPM ≥ 1), most of

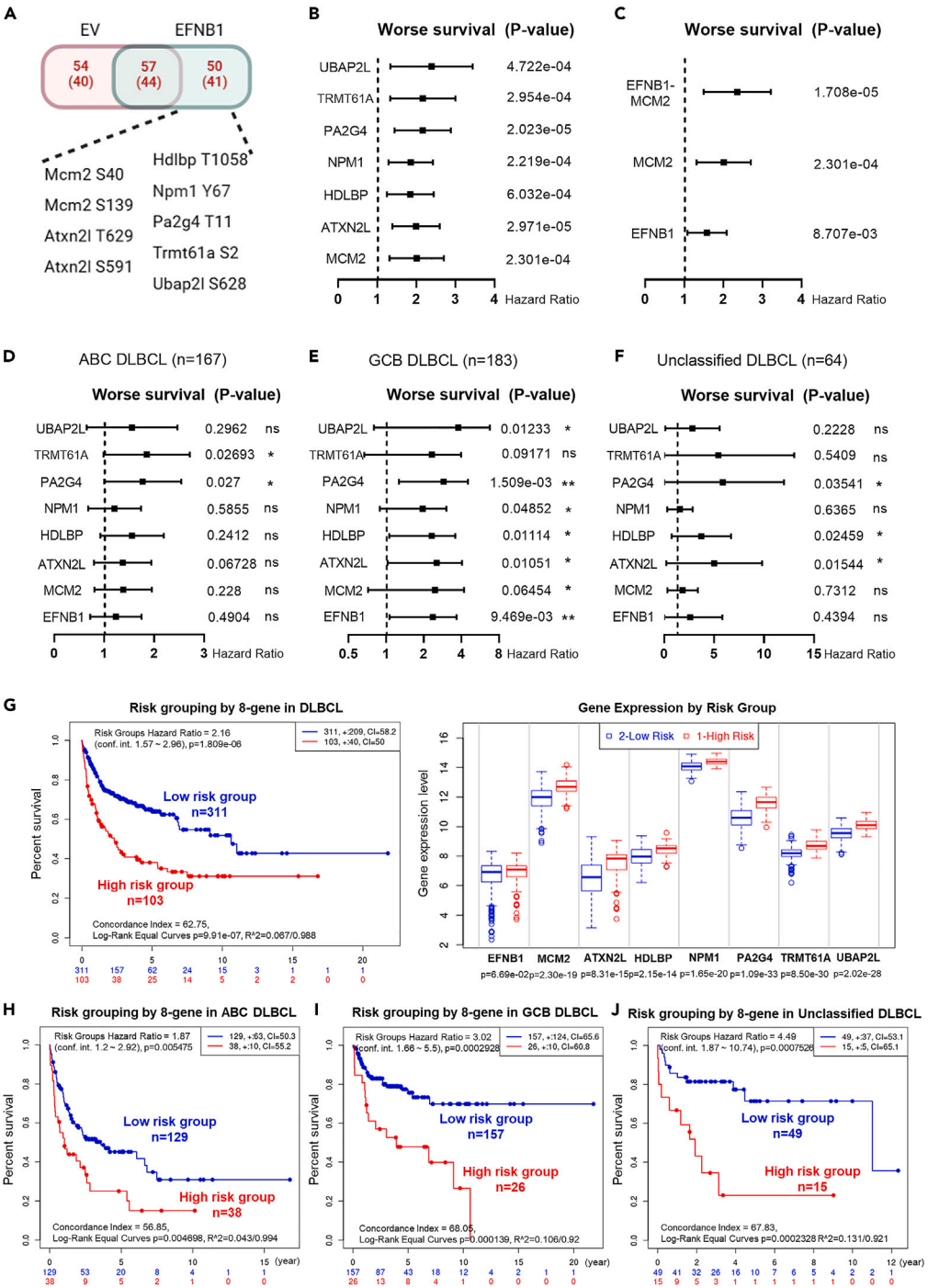

Figure 4. The EFNB1 phosphorylation signaling network is associated with the prognosis of GCB-DLBCL

(A) Phosphorylated peptides/proteins identified in Efnb1 cells.

(B) Forest plot for the prognostic performance of indicated genes. p Value of the log rank test was shown. A human DLBCL dataset (Lenz-Staudt DLBCL GSE10846) was used for survival analysis. The hazard ratio (HR), confidence interval, p Value in the forest plot were obtained from the SurvExpress program. DLBCL, number of patients = 414.

(C) Forest plot for the prognostic performance of the individual and joint expression of EFNB1 and MCM2. p Value of the log rank test was shown.

(D–F) Forest plot for the prognostic performance of indicated genes in ABC DLBCL (D), GCB DLBCL (E), and UC DLBCL (F). ABC DLBCL, number of patients = 167. GCB DLBCL, number of patients = 183. UC DLBCL, number of patients = 64.

(G–J) Survival curve of DLBCL patients (G), ABC DLBCL patients (H), GCB DLBCL patients (I), Unclassified DLBCL patients (J) and the expression level of the 8 genes in low-risk and high-risk groups. The prognostic index (PI) was calculated by the joint expression level of the 8 genes and the Cox model to generate the risk groups. The optimization algorithm was applied in risk grouping.

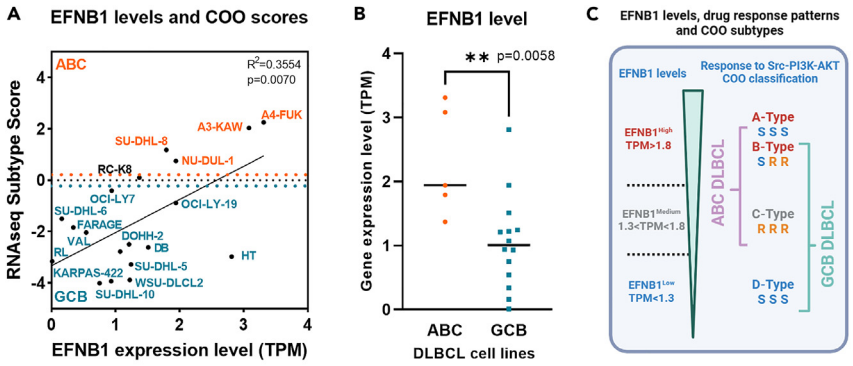

D

Cell lines	Efnb1(FPKM)	COOscore
EV-R1	0.15	1.13
EV-R2	0.02	1.11
Efnb1-R1	97.54	1.48
Efnb1-R2	91.56	1.27

E

Eμ-Myc lymphomas	Efnb1(FPKM)	COOscore	Cell of origin
Utx^{WT}-R1	0.24	1.19	pro-B
Utx^{WT}-R2	0.09	0.75	pro-B
Utx^{KO}-R1	10.64	1.59	mature B
Utx^{KO}-R2	50.48	1.62	mature B

Figure 5. EFNB1 level is a potential indicator for the degree of B-cell differentiation and activation

See also Table S3.

(A) The correlation of EFNB1 levels and COO scores in the DLBCL cell lines. The ABC cell lines are in yellow and the GCB cell lines are in cyan.

(B) The EFNB1 level in ABC and GCB cell lines.

(C) The relevance between EFNB1 level, COO score and drug response pattern in the DLBCL cell lines.

(D) Efnb1 levels and COO scores in Eμ-Myc; $Cdkn2a^{-/-}$ cells.

(E) Efnb1 levels, COO scores, cell of origin in Eμ-Myc lymphomas. Data are presented as mean ± SEM. *p < 0.05, **p < 0.01, ***p < 0.001, ****p < 0.0001 and n.s. indicates not significant (p > 0.05).

which are resistant B-Type and C-Type (Figure 5C). GCB cell lines are mainly EFNB1 $^{low\text{-}medium}$ cells (TPM ≤ 2), and sensitive D-Type are all included (Figure 5C). This difference provides a reasonable explanation for the correlation between EFNB1 level and GCB prognosis, rather than ABC prognosis. Overall, EFNB1 level is associated with cell of origin and COO score. Moreover, EFNB1 level is a potential quantitative indicator for the degree of B-cell differentiation.

Next, to investigate whether EFNB1 directly promotes B-cell differentiation, we calculated the COO scores of murine lymphoma cell lines and primary lymphomas. Due to differences in the expression of COO-related genes between mouse and human, here we only use the alteration of COO scores to evaluate the cell differentiation trends, rather than the GCB and ABC origins. In Eμ-Myc; $Cdkn2a^{-/-}$ cells, ectopic expression of EFNB1 increased the COO score by 12%–32% (Figure 5D), indicating that EFNB1 promotes cell differentiation toward the ABC/post-GC stage by regulating gene expression of the 20 COO-related genes. Similarly, Efnb1 is almost not expressed in Eμ-Myc lymphomas originated from the pro-B cell stage, with a COO score ranging from 0.75 to 1.19 (Figure 5E). However, Efnb1 level significantly increased to 10–50 (FPKM) in UTX knockout Eμ-Myc lymphomas originated from the mature B-cell stage, with COO score increasing to around 1.6 (Figure 5E). In addition, the highest level of endogenous EFNB1 in UTX-KO lymphoma is 50 (FPKM). The ectopic expression level of EFNB1 in Eμ-Myc; $Cdkn2a^{-/-}$ cell line is 91–97 (FPKM). The difference of twice should be in physiologically range. Together, consistent with the previous report that EFNB1 is a biomarker of GC-B cell,[21] these results support that EFNB1 promotes cell differentiation toward the ABC/post-GC stage and is a potential indicator for the degree of B-cell differentiation/activation.

EFNB1 level is associated with the prognosis of PCNSL patients

Our previous study showed that knockout of UTX can significantly increase EFNB1 expression and promote the occurrence of PCNSL. Therefore, we analyzed the transcriptome data from a recent PCNSL study[37] and found that the expression level of EFNB1 is associated with the prognosis of PCNSL (p = 0.0045) (Figure 6A). EFNB1 level is relatively low in the high-risk group and inversely correlated with COOscore (p = 0.0064) (Figures 6A and 6B), which is the opposite of what we observed in GCB-DLBCL, suggesting that EFNB1 may have a different mechanism in PCNSL. In addition, KDM6A (UTX) level is also associated with the prognosis of PCNSL (p = 0.0052) (Figure 6C). Furthermore, KDM6A expression is relatively low in the high-risk group (Figure 6C), which is consistent with what we observed in DLBCL, suggesting that KDM6A is also a potential tumor suppressor gene in PCNSL. However, unlike EFNB1, KDM6A level lacks correlation with COOscore (Figure 6D).

In summary, we found that the correlation between EFNB1 level and PCNSL prognosis or COO score is opposite to that observed in GCB-DLBCL, suggesting that EFNB1 may have different effects on pathological progression in different subtypes of B-cell lymphoma. It also should be noted that although PCNSL is also characterized by activation of the BCR signaling pathway, transcriptionally similar to ABC-DLBCL, PCNSL and DLBCL have their own unique transcriptional features and have been classified as two different subtypes in the latest 5th edition of the WTO classification.[38] Moreover, the survival time of PCNSL patients is much shorter than that of ABC-DLBCL patients, with most

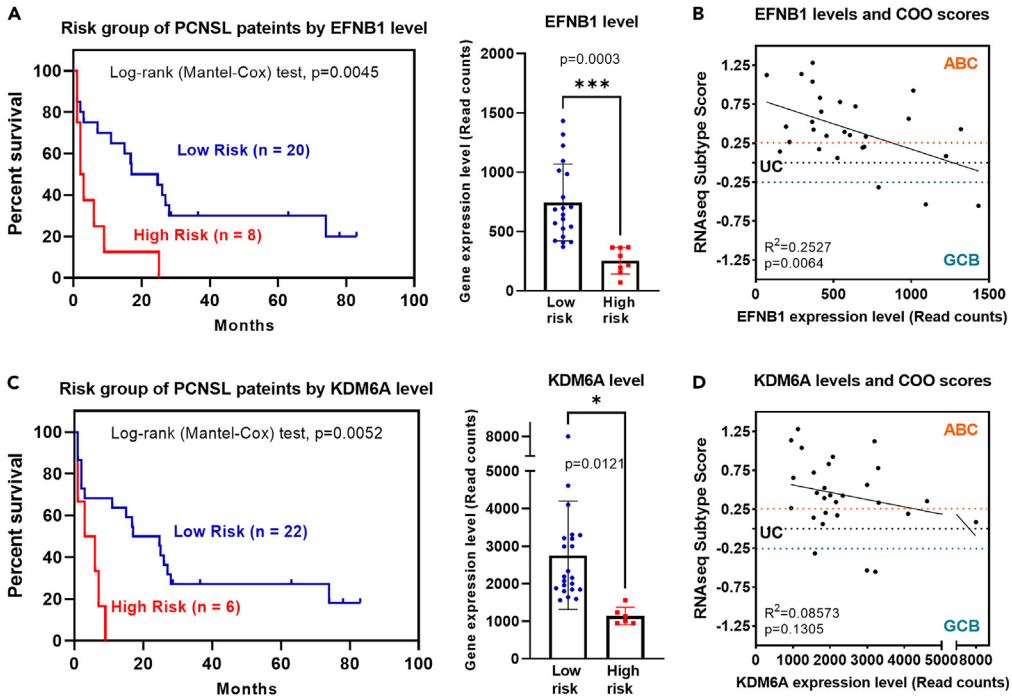

Figure 6. EFNB1 Level is associated with the prognosis of PCNSL patients

(A) Survival curve of PCNSL patients and EFNB1 levels in low-risk and high-risk groups. Number of patients in low-risk group = 20. number of patients in high-risk group = 8. Risk grouping was determined by the optimal significance difference.

(B) EFNB1 levels and COO scores in the PCNSL.

(C) Survival curve of PCNSL patients and KDM6A levels in low-risk and high-risk groups. Number of patients in low-risk group = 22. Number of patients in high-risk group = 6. Risk grouping was determined by the optimal significance difference.

(D) KDM6A levels and COO scores in the PCNSL. Data are presented as mean ± SEM. *p < 0.05, **p < 0.01, ***p < 0.001, ****p < 0.0001 and n.s. indicates not significant (p > 0.05).

patients surviving for less than 2 years (Figures 6A and 6C). Therefore, we believe that the significance of EFNB1 as a drug target is more important than its diagnostic value. We speculate that EFNB1 agonists may be a potential therapeutic agent for PCNSL.

EFNB1 levels are associated with drug response patterns of SRC-PI3K-AKT inhibitors in the BL and MM cell lines

Next, we further analyzed the expression of EFNB1 in two other subtypes of B-cell malignancies, BL and MM, as well as their drug response patterns. Eight BL cell lines and fifteen MM cell lines with available IC50 data were selected and analyzed (Table 2).

Ultimately, we identified two drug response patterns that were not present in DLBCL cell lines (Figures 7A and 7B), E-Type and F-Type, suggesting that BL and MM have completely different cell-dependency on the EFNB1-associated networks compared to DLBCL. Most BL cell lines (7/8) showed a unique E-Type pattern (Figure 7A), indicating that BL cell lines have a unique dependency related to E-Type pattern. Most EFNB1^{high} MM cell lines (7/8, TPM>2) showed the F-Type pattern and most EFNB1$^{medium\text{-}low}$ MM cell lines (5/7, TPM<2) showed the C-Type pattern (Figure 7B).

After calculating the COO score, we found that all BL cells have a similar transcriptome to the GCB-like or UC-like stage (Figure 7C, See Table S3), while all MM cells have a similar transcriptome to the ABC/post-ABC-like stage (Figure 7D, See Table S3). However, unlike DLBCL and PCNSL, EFNB1 level is not correlated with COO score in BL (p = 0.1961) and MM (p = 0.2606). A reasonable explanation is that BL and MM originate from the early and late stages of mature B-cell activation, respectively, and there is little difference in cell differentiation. We further found that GCB-DLBCL has the lowest EFNB1 level and is significantly different from other subtypes (Figure 7E). Finally, we summarized the EFNB1 level, COO score, drug response patterns, and potential therapeutic options in DLBCL, BL, and MM (Figure 7F). These results suggest that different subtypes of B-cell neoplasms have distinctive drug response patterns, which are associated with EFNB1 levels. EFNB1 level is a potential quantitative biomarker for predicting the COO of B-cell neoplasms and drug response patterns, which helps to determine the most effective treatment plan or drug combination.

The EFNB1 phosphorylation signaling network is associated with the prognosis of FL, MM, and CLL

Given the association between EFNB1 levels and the drug response patterns in B-cell neoplasms, we further investigated the prognostic relevance of EFNB1 and seven genes (MCM2, ATXN2L, HDLBP, NPM1, PA2G4, TRMT61A, UBAP2L) in other B-cell neoplasms. Follicular

Table 2. The classification and genetic status of BL and MM cell lines

Cell lines	Lineage sub-subtype	MSI status	Mutational Burden	Ploidy WES	Gender
BL-41	Burkitt's Lymphoma	MSS	25.58	2.16	Male
CA46	Burkitt's Lymphoma	MSS	30.42	2.11	Male
DAUDI	EBV-Related Burkitt's Lymphoma	MSS	1922.63	1.99	Male
GA-10	Burkitt's Lymphoma	MSS	34.74	2.04	Male
NAMALWA	EBV-Related Burkitt's Lymphoma	–	49.26	2.02	Female
RAJI	EBV-Related Burkitt's Lymphoma	MSS	32.21	2.09	Male
RAMOS	Burkitt's Lymphoma	MSS	30.89	2.04	Male
ST486	Burkitt's Lymphoma	MSS	30.34	2.13	Female
AMO-1	Plasma Cell Myeloma	MSS	40.42	3.68	Female
EJM	Plasma Cell Myeloma	MSS	55.79	3.06	Female
JJN-3	Plasma Cell Myeloma	MSS	28.37	2.80	Female
KARPAS-620	Plasma Cell Myeloma	MSS	20.5	3.08	Female
KMS-11	Plasma Cell Myeloma	MSS	54.45	3.25	Female
KMS-12-BM	Plasma Cell Myeloma	MSS	35.95	3.52	Female
L-363	Plasma Cell Myeloma	MSS	32.87	2.17	Female
LP-1	Plasma Cell Myeloma	MSS	28.68	3.56	Female
MM1S	Plasma Cell Myeloma	MSS	39.47	1.99	Female
MOLP-8	Plasma Cell Myeloma	MSS	39.39	2.10	Male
NCI-H929	Plasma Cell Myeloma	MSS	27.97	1.98	Female
OPM-2	Plasma Cell Myeloma	MSS	44.34	3.27	Female
RPMI-8226	Plasma Cell Myeloma	MSS	42.68	2.94	Male
SK-MM-2	Plasma Cell Myeloma	MSS	32.89	2.08	Male
U-266	Plasma Cell Myeloma	MSS	41.39	2.05	Male

Abbreviation: EBV, Epstein-Barr virus. MSI, microsatellite instability. MSS, microsatellite stability. WES, whole exon sequencing.

Lymphoma (FL) (Leich-Staudt, FL, GSE16131), MM (Shaughnessy, MM, GSE2658), Chronic Lymphocytic Leukemia (CLL) (Herold Bohlander, CLL, GSE22762), were used to perform survival analysis. The results showed that the expression levels of most EFNB1-associated genes were significantly associated with prognosis of FL, MM, CLL (Figures 8A–8C), suggesting that abnormality of the EFNB1 phosphorylation signaling network is common in B-cell neoplasms and contributes to the malignant progression of B-cell neoplasms.

Among the eight genes, HDLBP and UBAP2 were significantly associated with the prognosis of MM and CLL ($p < 0.001$, ***), suggesting that the biological functions involved in HDLBP and UBAP2 may play an important role in the malignant progression of MM and CLL. At the same time, the expression level of EFNB1 is not correlated with the prognosis of MM, suggesting that there are other mechanisms that can regulate the activation of the EFNB1 phosphorylation signaling network, thereby promoting malignant progression and drug response. Of course, expression regulation is not the only regulatory mechanism of gene function. Protein stability and post-translational modifications (PTMs) are also alternative regulatory mechanisms of gene function and need to be further investigated.

Next, we further analyzed the prognostic relevance of the 8-gene signature in three types of B-cell neoplasms. Survival curve analysis showed that the joint expression level of the eight genes can effectively distinguish high-risk and low-risk groups of FF (Figure 8D), MM (Figure 8E), and CLL (Figure 8F), suggesting that the abnormality of the EFNB1 phosphorylation signaling network is a common mechanism of malignant progression in various B-cell neoplasms.

In summary, the prognostic analysis suggests that the abnormality of the EFNB1 phosphorylation signaling pathway is closely related to the prognosis of B-cell malignancies, which may be one of the reasons for treatment failure. Genes involved in the EFNB1 phosphorylation signaling pathway are also the promising prognostic biomarkers.

The effect of EFNB1 on drug response is not EFNB1 level dependent

To analyze the effect of EFNB1 level on drug response, we further established several single-clone cell strains with decreased and increased GFP/EFNB1 from EFNB1-GFP transduced *Eμ-Myc;Cdkn2a*$^{-/-}$ cells (Figure 9A). Compared with the parental cell line, there was no significant difference in the sensitivity to targeted drugs and cytotoxic drug (dasatinib, MK-2206, doxorubicin) among the single-clone cell strains (Figure 9B). These results suggest that, unlike COO scores, the role of EFNB1 in regulating cell dependence and drug sensitivity should be cell background dependent rather than EFNB1 level dependent.

A Drug response profile of BL cell lines to kinase inhibitors

Cell line panel (BL)	EFNB1 (TPM)	ABL-SRC		ABL	BTK	SYK	panPI3K			panAKT			Drug Response Pattern
		Dasa	Bosu	Nilo	Ibru	Entosple	Tase	Picti	Bupar	MK-2206	Afure	Upro	
CA46	2.38	0.22	0.37	1.13	1.99	1.16	0.95	0.11	0.29	0.85	0.70	0.92	E-Type
BL41	2.23	0.52	0.70	0.96	1.32	1.23	1.12	0.36	0.27	1.13	0.71	0.86	E-Type
ST486	2.18	0.15	-	0.26	1.26	0.92	1.24	0.41	0.22	1.39	0.98	1.09	E-Type
GA10	2.06	-0.50	-0.03	0.21	0.52	0.05	0.11	-0.50	-0.04	-0.05	0.50	0.36	Others
RAJI	1.97	0.88	0.84	0.00	2.07	1.37	1.66	0.73	0.28	1.04	1.09	1.42	E-Type
DAUDI	1.59	0.37	0.31	1.54	2.05	1.34	0.71	0.45	0.49	0.79	0.90	0.86	E-Type
NAMALWA	1.09	0.24	0.48	1.14	0.84	0.44	-0.08	-0.11	0.11	0.67	0.22	0.27	E-Type
RAMOS	0.45	0.49	0.72	0.63	1.82	1.59	1.12	0.45	0.35	0.95	0.63	0.79	E-Type

Log_{10}(IC50) Sensitivity ← -0.5 | 0 | 0.5 | 1 | 1.5 → Resistance

B Drug response profile of MM cell lines to kinase inhibitors

Cell line panel (MM)	EFNB1 (TPM)	ABL-SRC		ABL	BTK	SYK	panPI3K			panAKT			Drug Response Pattern
		Dasa	Bosu	Nilo	Ibru	Entosple	Tase	Picti	Bupar	MK-2206	Afure	Upro	
KARPAS-620	13.67	0.93	1.21	1.18	1.18	2.11	-0.14	0.08	0.29	0.23	0.17	0.02	F-Type
KMS-11	6.87	0.44	0.96	0.67	1.32	1.22	-0.67	-0.40	0.04	-0.20	0.23	0.37	F-Type
L-363	4.02	0.76	0.48	0.66	1.92	1.16	0.18	0.31	-0.26	0.49	0.15	0.28	F-Type
OPM-2	3.84	0.56	0.50	1.20	1.35	1.32	0.14	0.46	0.24	0.46	-0.02	0.37	F-Type
LP-1	2.84	1.23	1.68	2.26	2.32	2.51	1.65	1.03	0.48	1.39	1.26	1.78	C-Type
AMO-1	2.82	0.45	0.66	0.69	1.43	0.77	0.09	0.07	-0.33	0.35	0.35	0.61	F-Type
MM1S	2.37	1.14	0.48	1.13	1.75	1.93	-0.89	-0.41	-0.03	-0.55	-0.65	-0.69	F-Type
MOLP-8	2.26	0.32	0.47	1.13	2.01	1.91	-0.76	-0.50	0.18	-0.05	0.92	0.14	F-Type
JJN-3	1.99	1.00	0.56	0.76	1.99	1.66	1.12	0.76	0.18	1.12	1.00	1.78	C-Type
RPMI-8226	1.91	0.84	0.71	1.27	1.32	0.96	0.89	0.64	0.25	0.92	1.31	1.02	C-Type
SK-MM-2	1.84	1.70	0.84	2.04	2.52	2.14	1.01	0.92	0.99	1.35	0.93	1.58	C-Type
NCI-H929	1.69	0.28	0.46	0.58	2.09	1.24	-1.68	-0.95	-0.42	-1.11	-1.12	-1.12	F-Type
EJM	1.06	1.03	0.94	1.14	2.16	1.78	0.93	0.51	0.74	0.94	1.25	1.38	C-Type
U-266	0.5	0.86	1.11	1.56	2.27	1.86	1.73	1.26	1.05	1.99	2.11	2.10	C-Type
KMS-12-BM	0.25	0.44	0.37	0.78	1.91	1.33	-0.02	-0.25	-0.17	-0.06	0.49	1.21	F-Type

Log_{10}(IC50) Sensitivity ← -0.5 | 0 | 0.5 | 1 | 1.5 → Resistance

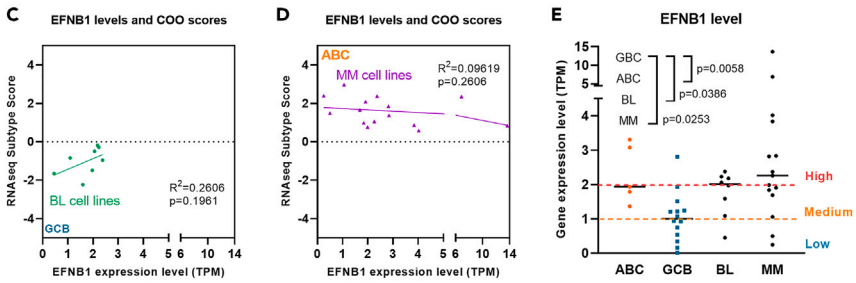

F The correlation of EFNB1 levels, COO scores, drug response patterns, potential treatment options in DLBCL, BL, MM.

Mature B Neoplasms	EFNB1 levels (TPM)	COO Scores	Drug Response Patterns	Sensitivity/Resistance			Potential treatment options
				SRC	PI3K	AKT	
DLBCL	High (1.94-3.31) Medium (1.37-1.79) Low (0.16-1.24)	High & Medium: GCB or ABC Low: GCB	A-Type	S	S	S	High: SRCi, PI3Ki/AKTi Medium: Others
			B-Type	S	R	R	
			C-Type	R	R	R	
			D-Type	S	S	S	Low: R-CHOP
BL	High (2-2.4) Medium (1-2)	GCB-like	E-Type	S	S	R	High & Medium: SRCi, PI3Ki
MM	High (2-7) Medium (1-2)	ABC-like	F-Type	R	S	S	High: PI3Ki/AKTi Medium: Others
			C-Type	R	R	R	

Figure 7. EFNB1 levels are associated with drug response patterns of SRC-PI3K-AKT inhibitors in the BL and MM cell lines

See also Table S3.

(A and B) Drug response profile of targeted drugs in the BL (A) and MM (B) cell lines. Efnb1 levels were evaluated by TPM. TPM, Transcripts Per Kilobase per Million mapped reads. Drug response was evaluated by IC50, the half maximal inhibitory concentration. The unit for IC50 is μM. Dasa, Dasatinib. Bosu, Bosutinib. Nilo, Nilotinib. Ibru, Ibrutinib. Entosple, Entospletinib. Tase, Taselisib. Picti, Pictilisib. Bupar, Buparlisib. Afure, Afuresertib. Upro, Uprosertib. E-Type pattern was identified in BL cell lines. F-Type and C-Type patterns were identified in the EFNB1^{high} and EFNB1$^{medium\text{-}low}$ MM cell lines, respectively.

(C and D) The correlation of EFNB1 levels and COO scores in the BL (C) and MM (D) cell lines. The BL cell lines are in green and the MM cell lines are in roseo.

(E) The expression level of EFNB1 in ABC-DLBCL, GCB-DLBCL, BL, and MM.

(F) The correlation of EFNB1 levels, COO scores, drug response patterns, and potential treatment options in DLBCL, BL, MM. Data are presented as mean ± SEM. *p < 0.05, **p < 0.01, ***p < 0.001, ****p < 0.0001 and n.s. indicates not significant (p > 0.05).

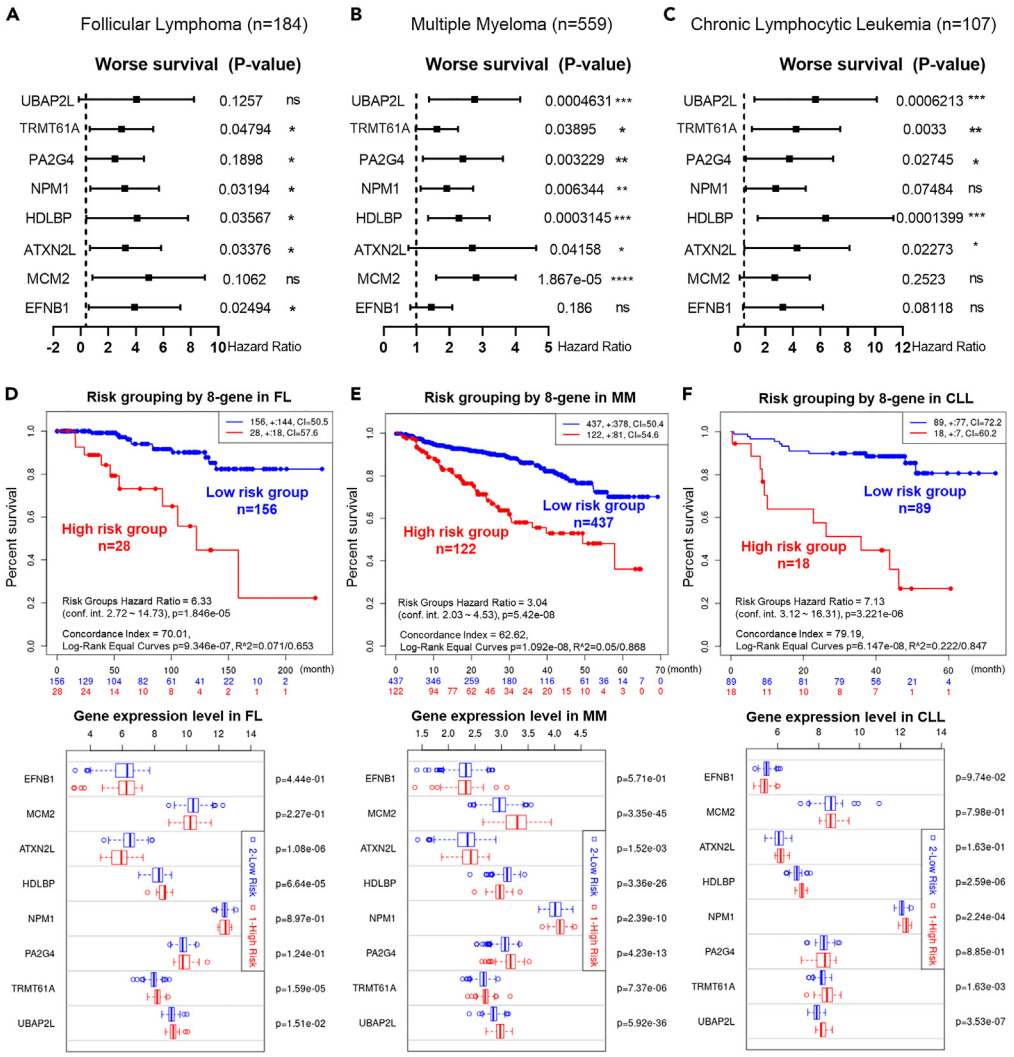

Figure 8. The EFNB1 phosphorylation signaling network is associated with the prognosis of FL, MM, and CLL

(A–C) Forest plot for the prognostic performance of indicated genes in FL (A), MM (B), and CLL (C). The following datasets Leich-Staudt FL GSE16131, Shaughnessy MM GSE2658, Herold Bohlander CLL GSE22762 were used for survival analysis. p Value of the log rank test was shown. The hazard ratio (HR), confidence interval, p Value in the forest plot were obtained from the SurvExpress program. FL, number of patients = 184. MM, number of patients = 559. CLL, number of patients = 107.

(D–F) Survival curve of FL patients (D), MM patients (E), CLL patients (F) and the expression level of the 8 genes in low-risk and high-risk groups. The prognostic index (PI) was calculated by the joint expression level of the 8 genes and the Cox model to generate the risk groups. The optimization algorithm was applied in risk grouping.

In addition, we demonstrated that although single-clone derived cell lines with same genetic background is an ideal model to analyze the dose effect of individual gene expression levels. However, the discovery of EFNB1 levels and their drug response patterns may be cell background dependent, rather than cells with the same background. Hence, we speculated that endogenous EFNB1 levels and their specific cell features, such as cell of origin and signaling network, together determine cell dependency and drug response patterns.

DISCUSSION

Although targeted therapies have greatly improved the outcomes of DLBCL patients, the identification of predictive biomarkers for drug response is still challenging. Many multi-omics studies have accumulated mass of clinical cancer multi-omics data, of which patient prognosis is the most relevant to disease progression and drug efficacy. If the differences in gene expression or genetic variations are associated with the prognosis of patients, they are more likely to directly participate in drug response.

In this study, six drug response patterns of BCR associated kinase inhibitors SRC/PI3K/AKT were identified in human DLBCL, BL, and MM cell lines (Figure 10A). These six drug response patterns are correlated with the level of endogenous EFNB1 in cells. Among them, A/B-Type

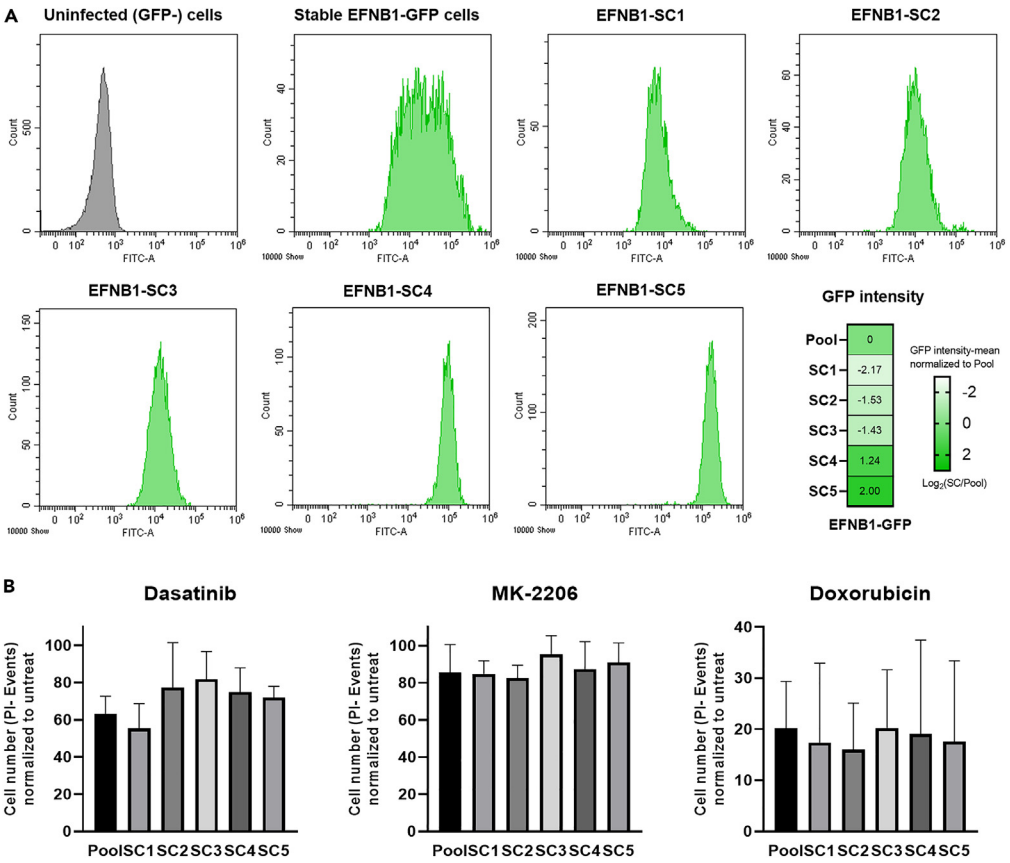

Figure 9. The effect of EFNB1 on drug response is dose-independent

(A) Establishment of five single-clone cell strains with decreased and increased GFP intensity.

(B) Inhibitory effect of drug treatment on cell proliferation in the parental pool cell line and single-clone cell strains. Cell counting is measured by flow cytometry analysis of PI negative cells at 48 h of the treatment. Dasatinib, 5μM. MK-2206, 5μM. Doxorubicin, 20nM. PI, propidium iodide. Data are obtained from three independent biological replicates. Data are presented as mean ± SEM. *p < 0.05, **p < 0.01, ***p < 0.001, ****p < 0.0001 and n.s. indicates not significant (p > 0.05).

and C-Type patterns appear in the EFNB1^{high} and EFNB1^{medium} DLBCL cell lines, respectively. D-Type pattern appears in the EFNB1^{low} DLBCL cell lines. E-Type pattern appears in the BL cell lines. F-Type pattern appears in the EFNB1$^{high\text{-}medium}$ MM cell lines. In addition, C-Type pattern also appears in the EFNB1^{low} MM cell lines. Moreover, the correspondence analysis of gene levels – drug response patterns suggested that EFNB1 level is a specific indicator of drug response patterns in human DLBCL cell lines. These findings reveal that the expression level of EFNB1 is correlated with the dependency of cells on BCR-related kinases, suggesting that EFNB1 is a promising biomarker for the efficacy evaluation and prediction of targeted drugs.

Using *Eμ-Myc;Cdkn2a−/−* cell model, we demonstrated that ectopic expression of Efnb1 conferred cells sensitivity to SRC inhibitors and most cytotoxic drugs. Mechanically, Efnb1-induced phosphorylation may largely increase the dependency of cells on the SRC signaling pathway, which sensitizes cells to SRC inhibitors (Figure 10A). Moreover, Efnb1-induced phosphorylation of Stmn1 at serine 28 confers cells hypersensitivity to vincristine (Figure 10A). In addition, the EFNB1 phosphorylation signaling network identified by mass spectrometry was significantly correlated with the prognosis of GCB-DLBCL, suggesting that the phosphorylation signaling network induced by EFNB1 is involved in the pathological progression of DLBCL. In addition, although the expression level of endogenous EFNB1 in Eμ-Myc; Cdkn2a$^{-/-}$ cells is very low, due to the high lethal dose of most targeted drugs, usually over 20 μmol, the Eμ-Myc; Cdkn2a$^{-/-}$ cell model should be classified as C-Type pattern, multi-inhibitor tolerant. Efnb1-overexpression cells should be classified as B-Type, as Efnb1-overexpression leads to sensitivity to SRC inhibitors and no difference in PI3K-AKT inhibitors.

Ectopic expression of EFNB1 confers cells sensitivity to SRC inhibitors, indicating that SRC is a key kinase for cell survival and proliferation, and EFNB1 can regulate the activity of SRC. However, the relationship between EFNB1 levels and SRC phosphorylation has not been validated in human DLBCL cell lines (Figure S1). Moreover, there is no differences on drug response in single-clone cell strains with differential GFP/EFNB1 level, suggesting that the differences on drug response patterns in human DLBCL cell lines are cell background dependent (Figure 9). Due to the high heterogeneity, there may be multiple mechanisms by which EFNB1 regulates BCR-related kinase activity and its cell-dependent effects in different B-cell neoplasm cell lines. The dependence of cell proliferation and survival on specific pathways and kinases,

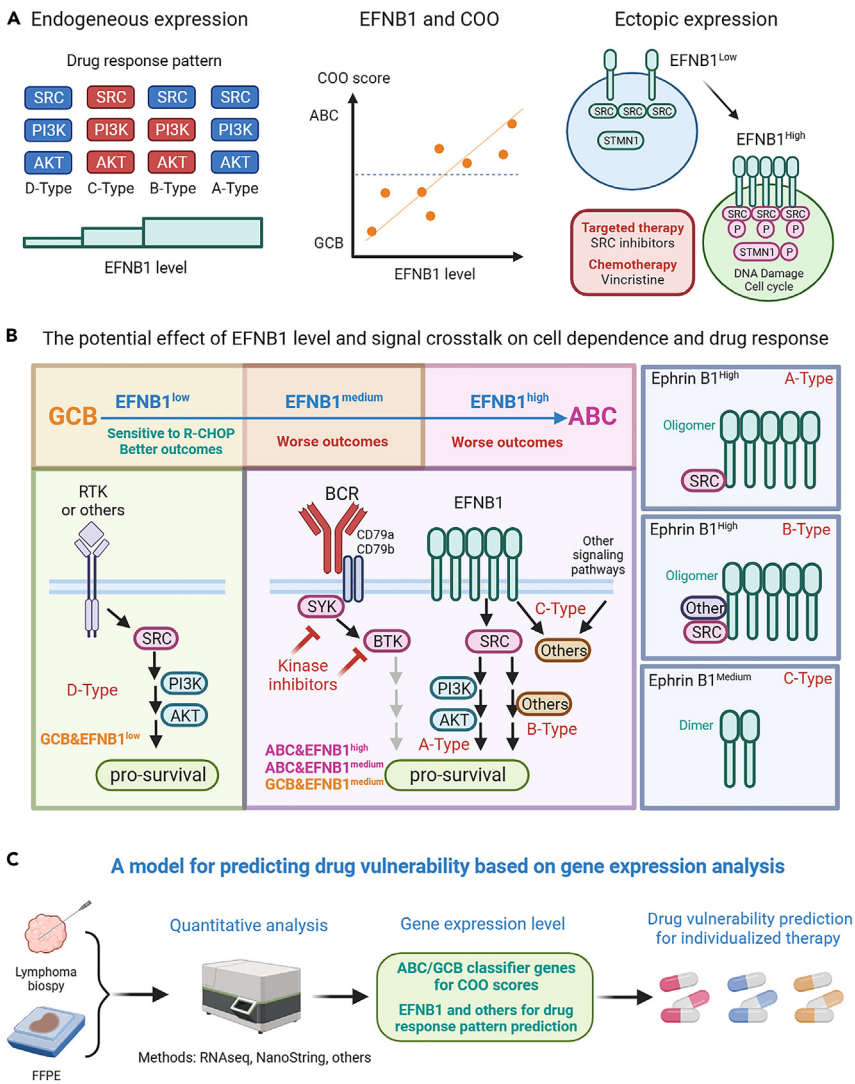

Figure 10. Hypothesis of EFNB1 levels regulating drug response patterns and its clinical implication

(A) The correlation between endogenous EFNB1 levels and the classification of B-cell neoplasms, cell of origin, drug response patterns, prognosis, and the role of ectopic expression of EFNB1.

(B) Different levels of EFNB1 form multiple aggregates that crosstalk with the BCR signaling network, maintaining pro-proliferative signals and causing differences in cell dependency on the SRC/PI3K/AKT signaling network.

(C) Quantitative analysis of EFNB1 levels as a model for guiding lymphoma classification, prognostic predication, and efficacy evaluation.

and whether the cell is sensitive to inhibitors of the kinases/pathways, are two different issues. Different cells can depend on the same signaling pathways, but their sensitivity to inhibitors may be different (Figure 10B). For example, the BCR signaling in ABC cells is activated, and the survival and proliferation of ABC cells are highly dependent on BCR signaling. However, some ABC cells are not sensitive to BCR signaling inhibitors, such as the BTK inhibitor. One explanation is that the BCR signaling pathway is overactivated, and a single BTKi inhibitor still cannot block the BCR signaling pathway (Figure 10B). Another explanation is that the BCR signaling pathway is not the only signaling pathway that maintains cell survival and proliferation (Figure 10B). When the BCR signaling pathway is blocked, cells can still depend on other pro-proliferative signaling pathways, resulting in tolerance to the BTKi inhibitor.

Kinase inhibitors such as BTKi and PI3Ki have been approved for the treatment of various B-cell malignancies, but resistance can occur through multiple mechanisms, such as complementary pro-survival signaling pathways.[13] The crosstalk among pro-survival signaling pathways, such as Eph-Ephrin and RTK,[39] greatly weakens the cell's dependency on a single signaling pathway or a single kinase, leading to the tolerance of targeted drugs. Combination therapy with multiple kinase inhibitors is one of the feasible strategies to overcome kinase inhibitor resistance. It is worth further exploring whether the level of EFNB1 changes during the process of treatment and acquired drug resistance, thus serving as a predictive biomarker for drug resistance.

The correspondence analysis of EFNB1 levels – drug responses in human DLBCL cell lines shows that EFNB1^{low} cell lines are generally sensitive to most targeted drugs, indicating a strong dependence of EFNB1^{low} cells on BCR and PI3K-AKT signaling pathways. Contrary to EFNB1^{low} cell lines, EFNB1^{medium} cell lines are tolerant to most targeted inhibitors, indicating that the survival of EFNB1^{medium} cell lines is not dependent on the BCR and PI3K-AKT signaling pathways. However, in EFNB1^{high} cell lines, the correspondence between EFNB1 level and drug response is very complicated, with some cell lines showing sensitivity to PI3K-ATK inhibitors. Meanwhile, these drug response patterns observed in the DLBCL cell lines are also partially supported by the protein and phosphoproteins expression of cancer signaling pathways (Figure S1). These results suggest that different levels of EFNB1 are associated with different signaling networks and dependencies. An explanation for the diversity of EFNB1 phosphorylation signaling network in different cells was the diversity of Ephrin aggregates. Ephrins, as the ligands for Eph receptors, can form dimers and oligomers and activate bidirectional signaling pathways through their interaction with Eph receptors. Meanwhile, it is worth noting that Ephrins or Ephs can also be activated independently by self-polymerization or interaction with other signaling proteins.[23,40] We hypothesize that the activation of EFNB1 in DLBCL is Ephs independent. When EFNB1 within cells is at a moderate level, it can form dimers or small aggregates, which can trigger distinctive signaling networks other than the BCR and PI3K-AKT signaling pathways (Figure 10B). Hence, EFNB1^{medium} cell lines are tolerant to BCR and PI3K-AKT inhibitors. When EFNB1 in cells is at a high level, EFNB1 can form larger aggregates, allowing for the residence of more signaling proteins. Hence, SRC or other proteins, such as PI3K-AKT, are engaged as the pro-survival signaling pathways in EFNB1^{high} cell lines (Figure 10B).

The Eph-Ephrin signaling pathway is abnormally activated in various cancers, and targeting the Eph-Ephrin signaling pathway is a potential anti-tumor strategy.[41,42] However, due to the complementarity of the pro-survival signals, targeting Eph-Ephrin alone does not effectively inhibit tumor growth. Our results preliminarily found that overexpression of EFNB1 can sensitize cells to various cytotoxic drugs. Mass spectrometry data also supports that EFNB1 activates cytotoxic drug-related signaling pathways, such as DNA repair and cell cycle. Therefore, EFNB1 is expected to become a target for chemotherapy sensitizers. EFNB1 agonists are expected to be combined with cytotoxic drugs to reduce the dose and side effects of cytotoxic drugs.

Compared with DLBCL cell lines, BL and MM cell lines exhibit distinctive the correlation between drug response patterns and EFNB1 levels, suggesting that EFNB1 plays different roles in the pathological processes of different subtypes of B-cell neoplasms. These findings also suggested that the SRC/PI3K/AKT pattern can be used as a potentially functional classification indicator for different subtypes of B-cell neoplasms. High-throughput quantification methods, such as RNA-seq, although not currently a clinical routine method, have a large amount of information and sequencing costs continue to decline, making it an important technological development direction for precise diagnosis in the present and future. For example, two studies have performed high-throughput quantitative methods, the NanoString-based assay[35] and RNA-seq,[36] to analyze ABC/GCB types using FFPE tissue. Considering its correlation with drug response patterns, we proposed that quantitative analysis of EFNB1 levels may help distinguish different subtypes of B-cell neoplasms and predict their drug response patterns (Figure 10C). Our murine lymphoma/cell line data standardized by FPKM (0–97) is differently from publicly available human cell line data standardized by TPM (0–3.3). Moreover, EFNB1 levels in PCNSL data are standardized by Read Counts. Due to different methods of data standardization, we cannot compare the differences between different data. However, the range and relative expression level of EFNB1 expression differences within the same data should be evaluable.

In addition, we found that EFNB1 levels are associated with the origin of B-cell neoplasms. Cell of origin is a key basis for the classification of B-cell neoplasms, which is related to patient prognosis and also a hot topic in the pathological mechanism of B-cell lymphoma. BL and GCB-DLBCL originate from the GC stage, while ABC-DLBCL originates from the ABC/post-GC stage, among which ABC has the worst prognosis. We found that EFNB1 expression level can further divide GCB-DLBCL into high expression with poor prognosis and low expression with good prognosis subgroups, reflecting the potential of EFNB1 level as a prognostic marker for subtype classification. At the same time, cell models with ectopic expression of Efnb1 and lymphoma models with endogenous high expression of Efnb1 both show that EFNB1 can promote the increase of COO scores and differentiation toward ABC-like direction, suggesting that the increase of EFNB1 expression is the cause rather than the result of lymphoma progression. Therefore, we proposed that EFNB1 is not only a GC/postGC-specific gene with biological functions related to GC/postGC stage, but also that EFNB1 level, similar to COO score, can reflect the degree of cell differentiation in DLBLC and PCNSL.

Drug response, tumorigenesis, and prognosis are three distinct but closely related concepts of tumor progressions. Tumor progression is a dynamic process, and EFNB1 may play different roles in different B-cell neoplasms and different stages of tumor progression. Rapid disease progression and treatment failure/drug resistance are both causes of poor prognosis and are difficult to distinguish. For example, high-dose MTX and Ara-C are the main drugs in the R-HyperCVAD regimen in PCNSL, and relatively low expression of EFNB1 may promote the progression of PCNSL, or it may confer tumor cell resistance to MTX/Ara-C. Therefore, it is difficult to accurately determine the cause of poor prognosis in PCNSL with low expression of EFNB1, and rigorous experimental studies and retrospective analysis of clinical data may provide evidence to understand the role of EFNB1 in B-cell neoplasms.

This study uncovers a significant correlation between the expression level of EFNB1 and drug response. EFNB1 can regulate the phosphorylation of key molecules involved in drug response, such as SRC and STMN1, conferring sensitivity of cells to targeted and cytotoxic drugs. Our findings highlight the clinical implication of non-genetic biomarkers in drug efficacy prediction. In addition, we proposed that the expression level of key genes that are associated with malignant characteristics and worse outcomes may have more clinical significance than genetic classification biomarkers and should be given more attention.

Limitations of the study

Evaluating tumor heterogeneity and its impact on drug response is very challenging. This study focused on the analysis of cell lines and their drug response data. Although this study established an EFNB1 ectopic expression cell model and validated the role of EFNB1 in drug

response, and preliminarily explored its phosphorylation signaling network and clinical significance, it has not yet explored the impact of differences in endogenous expression levels and cell background on drug response. At the same time, this study was unable to obtain clinical trial data and perform retrospective validation of the drug response patterns observed in cell lines. The clinical study of efficacy prediction of EFNB1 levels requires rigorous design and systematic analysis. In addition, multiple factors can affect efficacy evaluation, and heterogeneous lymphoma animal models rather than heterogeneous cell line models should be the ideal model for comprehensive evaluation of drug efficacy.

STAR★METHODS

Detailed methods are provided in the online version of this paper and include the following:

- KEY RESOURCES TABLE
- RESOURCE AVAILABILITY
  - Lead contact
  - Materials availability
  - Data and code availability
- EXPERIMENTAL MODEL AND STUDY PARTICIPANT DETAILS
  - For cell lines
- METHOD DETAILS
  - Data acquisition and correspondence analysis
  - RPPA data analysis
  - Constructs
  - Chemicals
  - Drug response analysis
  - Western blot analysis
  - Mass spectrometry data analysis
  - Pathway enrichment analysis
  - Prognostic analysis
  - COO classification
- QUANTIFICATION AND STATISTICAL ANALYSIS

SUPPLEMENTAL INFORMATION

Supplemental information can be found online at https://doi.org/10.1016/j.isci.2023.108667.

ACKNOWLEDGMENTS

This work was supported by the National Natural Science Foundation of China (Grant Number 81900200) and the Natural Science Foundation of Jiangsu Province (Grant Number BK20190840). We acknowledge BioRender as the schematic figures in this manuscript were created using BioRender.com.

AUTHOR CONTRIBUTIONS

Conceptualization, X.L. and H.Q.; Methodology, X.L.; Software, X.L.; Validation, X.L., C.Z., M.D., and Y.J.; Formal analysis, X.L; Investigation, X.L., C.Z., M.D., and Y.J.; Resources, X.L. and Z.H.; Data curation, X.L., Y.J., and Z.H.; Writing – Original Draft, X.L.; Writing—Review and Editing, X.L. and H.Q.; Visualization, X.L.; Supervision, X.L.; Project Administration, X.L.; Funding Acquisition, X.L. All authors have read and agreed to the published version of the manuscript.

DECLARATION OF INTERESTS

The authors declare no conflict of interest.

INCLUSION AND DIVERSITY

We support inclusive, diverse, and equitable conduct of research.

Received: August 9, 2023
Revised: October 30, 2023
Accepted: December 5, 2023
Published: December 7, 2023

REFERENCES

1. Sehn, L.H., and Salles, G. (2021). Diffuse Large B-Cell Lymphoma. N. Engl. J. Med. *384*, 842–858.
2. Crombie, J., and LaCasce, A. (2021). The treatment of Burkitt lymphoma in adults. Blood *137*, 743–750.
3. Olszewski, A.J., Kurt, H., and Evens, A.M. (2022). Defining and treating high-grade B-cell lymphoma, NOS. Blood *140*, 943–954.
4. Ok, C.Y., and Medeiros, L.J. (2020). High-grade B-cell lymphoma: a term re-purposed in the revised WHO classification. Pathology *52*, 68–77.
5. Alizadeh, A.A., Eisen, M.B., Davis, R.E., Ma, C., Lossos, I.S., Rosenwald, A., Boldrick, J.C., Sabet, H., Tran, T., Yu, X., et al. (2000). Distinct types of diffuse large B-cell lymphoma identified by gene expression profiling. Nature *403*, 503–511.
6. Wright, G.W., Huang, D.W., Phelan, J.D., Coulibaly, Z.A., Roulland, S., Young, R.M., Wang, J.Q., Schmitz, R., Morin, R.D., Tang, J., et al. (2020). A Probabilistic Classification Tool for Genetic Subtypes of Diffuse Large B Cell Lymphoma with Therapeutic Implications. Cancer Cell *37*, 551–568.e14.
7. Weissinger, S.E., Dugge, R., Disch, M., Barth, T.F., Bloehdorn, J., Zahn, M., Marienfeld, R., Viardot, A., and Möller, P. (2022). Targetable alterations in primary extranodal diffuse large B-cell lymphoma. EJHaem *3*, 688–697.
8. Wilson, W.H., Young, R.M., Schmitz, R., Yang, Y., Pittaluga, S., Wright, G., Lih, C.-J., Williams, P.M., Shaffer, A.L., Gerecitano, J., et al. (2015). Targeting B cell receptor signaling with ibrutinib in diffuse large B cell lymphoma. Nat. Med. *21*, 922–926.
9. Salles, G., Schuster, S.J., de Vos, S., Wagner-Johnston, N.D., Viardot, A., Blum, K.A., Flowers, C.R., Jurczak, W.J., Flinn, I.W., Kahl, B.S., et al. (2017). Efficacy and safety of idelalisib in patients with relapsed, rituximab- and alkylating agent-refractory follicular lymphoma: a subgroup analysis of a phase 2 study. Haematologica *102*, e156–e159.
10. Lionakis, M.S., Dunleavy, K., Roschewski, M., Widemann, B.C., Butman, J.A., Schmitz, R., Yang, Y., Cole, D.E., Melani, C., Higham, C.S., et al. (2017). Inhibition of B Cell Receptor Signaling by Ibrutinib in Primary CNS Lymphoma. Cancer Cell *31*, 833–843.e5.
11. Grommes, C., Pastore, A., Palaskas, N., Tang, S.S., Campos, C., Schartz, D., Codega, P., Nichol, D., Clark, O., Hsieh, W.-Y., et al. (2017). Ibrutinib Unmasks Critical Role of Bruton Tyrosine Kinase in Primary CNS Lymphoma. Cancer Discov. *7*, 1018–1029.
12. Wilson, W.H., Wright, G.W., Huang, D.W., Hodkinson, B., Balasubramanian, S., Fan, Y., Vermeulen, J., Shreeve, M., Lm, S., and Staudt, L.M. (2021). Effect of ibrutinib with R-CHOP chemotherapy in genetic subtypes of DLBCL. Cancer Cell *39*, 1643–1653.e3.
13. Ondrisova, L., and Mraz, M. (2020). Genetic and Non-Genetic Mechanisms of Resistance to BCR Signaling Inhibitors in B Cell Malignancies. Front. Oncol. *10*, 591577.
14. Carrasco, Y.R., and Batista, F.D. (2006). B-cell activation by membrane-bound antigens is facilitated by the interaction of VLA-4 with VCAM-1. EMBO J. *25*, 889–899.
15. Chang, B.Y., Francesco, M., De Rooij, M.F.M., Magadala, P., Steggerda, S.M., Huang, M.M., Kuil, A., Herman, S.E.M., Chang, S., Pals, S.T., et al. (2013). Egress of CD19+CD5+ cells into peripheral blood following treatment with the Bruton tyrosine kinase inhibitor ibrutinib in mantle cell lymphoma patients. Blood *122*, 2412–2424.
16. Pasquale, E.B. (2008). Eph-Ephrin Bidirectional Signaling in Physiology and Disease. Cell *133*, 38–52.
17. Pasquale, E.B. (2010). Eph receptors and ephrins in cancer: bidirectional signalling and beyond. Nat. Rev. Cancer *10*, 165–180.
18. Miao, H., Li, D.-Q., Mukherjee, A., Guo, H., Petty, A., Cutter, J., Basilion, J.P., Sedor, J., Wu, J., Danielpour, D., et al. (2009). EphA2 mediates ligand-dependent inhibition and ligand-independent promotion of cell migration and invasion via a reciprocal regulatory loop with Akt. Cancer Cell *16*, 9–20.
19. Bouché, E., Romero-Ortega, M.I., Henkemeyer, M., Catchpole, T., Leemhuis, J., Frotscher, M., May, P., Herz, J., and Bock, H.H. (2013). Reelin induces EphB activation. Cell Res. *23*, 473–490.
20. Bochenek, M.L., Dickinson, S., Astin, J.W., Adams, R.H., and Nobes, C.D. (2010). Ephrin-B2 regulates endothelial cell morphology and motility independently of Eph-receptor binding. J. Cell Sci. *123*, 1235–1246.
21. Laidlaw, B.J., Schmidt, T.H., Green, J.A., Allen, C.D.C., Okada, T., and Cyster, J.G. (2017). The Eph-related tyrosine kinase ligand Ephrin-B1 marks germinal center and memory precursor B cells. J. Exp. Med. *214*, 639–649.
22. Lu, P., Shih, C., and Qi, H. (2017). Ephrin B1-mediated repulsion and signaling control germinal center T cell territoriality and function. Science *356*, eaai9264.
23. Kania, A., and Klein, R. (2016). Mechanisms of ephrin–Eph signalling in development, physiology and disease. Nat. Rev. Mol. Cell Biol. *17*, 240–256.
24. Li, X., Zhang, Y., Zheng, L., Liu, M., Chen, C.D., and Jiang, H. (2018). UTX is an escape from X-inactivation tumor-suppressor in B cell lymphoma. Nat. Commun. *9*, 2720–2810.
25. Shilts, J., Severin, Y., Galaway, F., Müller-Sienerth, N., Chong, Z.-S., Pritchard, S., Teichmann, S., Vento-Tormo, R., Snijder, B., and Wright, G.J. (2022). A physical wiring diagram for the human immune system. Nature *608*, 397–404.
26. Jiang, H., Pritchard, J.R., Williams, R.T., Lauffenburger, D.A., and Hemann, M.T. (2011). A mammalian functional-genetic approach to characterizing cancer therapeutics. Nat. Chem. Biol. *7*, 92–100.
27. Bruno, P.M., Liu, Y., Park, G.Y., Murai, J., Koch, C.E., Eisen, T.J., Pritchard, J.R., Pommier, Y., Lippard, S.J., and Hemann, M.T. (2017). A subset of platinum-containing chemotherapeutic agents kills cells by inducing ribosome biogenesis stress. Nat. Med. *23*, 461–471.
28. Palmer, A., Zimmer, M., Erdmann, K.S., Eulenburg, V., Porthin, A., Heumann, R., Deutsch, U., and Klein, R. (2002). EphrinB phosphorylation and reverse signaling: regulation by Src kinases and PTP-BL phosphatase. Mol. Cell *9*, 725–737.
29. Georgakopoulos, A., Litterst, C., Ghersi, E., Baki, L., Xu, C., Serban, G., and Robakis, N.K. (2006). Metalloproteinase/Presenilin1 processing of ephrinB regulates EphB-induced Src phosphorylation and signaling. EMBO J. *25*, 1242–1252.
30. Li, J., Lu, Y., Akbani, R., Ju, Z., Roebuck, P.L., Liu, W., Yang, J.-Y., Broom, B.M., Verhaak, R.G.W., Kane, D.W., et al. (2013). TCPA: a resource for cancer functional proteomics data. Nat. Methods *10*, 1046–1047.
31. Burgess, D.J., Doles, J., Zender, L., Xue, W., Ma, B., McCombie, W.R., Hannon, G.J., Lowe, S.W., and Hemann, M.T. (2008). Topoisomerase levels determine chemotherapy response in vitro and in vivo. Proc. Natl. Acad. Sci. USA *105*, 9053–9058.
32. Rana, S., Maples, P.B., Senzer, N., and Nemunaitis, J. (2008). Stathmin 1: a novel therapeutic target for anticancer activity. Expert Rev. Anticancer Ther. *8*, 1461–1470.
33. Jun, H.J., Appleman, V.A., Wu, H.-J., Rose, C.M., Pineda, J.J., Yeo, A.T., Delcuze, B., Lee, C., Gyuris, A., Zhu, H., et al. (2018). A PDGFRα-driven mouse model of glioblastoma reveals a stathmin1-mediated mechanism of sensitivity to vinblastine. Nat. Commun. *9*, 1–13.
34. Lyu, J., Yang, E.J., Zhang, B., Wu, C., Pardeshi, L., Shi, C., Mou, P.K., Liu, Y., Tan, K., and Shim, J.S. (2020). Synthetic lethality of RB1 and aurora A is driven by stathmin-mediated disruption of microtubule dynamics. Nat. Commun. *11*, 5105–5116.
35. Scott, D.W., Wright, G.W., Williams, P.M., Lih, C.-J., Walsh, W., Jaffe, E.S., Rosenwald, A., Campo, E., Chan, W.C., Connors, J.M., et al. (2014). Determining cell-of-origin subtypes of diffuse large B-cell lymphoma using gene expression in formalin-fixed paraffin-embedded tissue. Blood *123*, 1214–1217.
36. Reddy, A., Zhang, J., Davis, N.S., Moffitt, A.B., Love, C.L., Waldrop, A., Leppa, S., Pasanen, A., Meriranta, L., Karjalainen-Lindsberg, M.-L., et al. (2017). Genetic and Functional Drivers of Diffuse Large B Cell Lymphoma. Cell *171*, 481–494.e15.
37. Radke, J., Ishaque, N., Koll, R., Gu, Z., Schumann, E., Sieverling, L., Uhrig, S., Hübschmann, D., Toprak, U.H., López, C., et al. (2022). The genomic and transcriptional landscape of primary central nervous system lymphoma. Nat. Commun. *13*, 2558.
38. Alaggio, R., Amador, C., Anagnostopoulos, I., Attygalle, A.D., Araujo, I.B.d.O., Berti, E., Bhagat, G., Borges, A.M., Boyer, D., Calaminici, M., et al. (2022). The 5th edition of the World Health Organization Classification of Haematolymphoid Tumours: Lymphoid Neoplasms. Leukemia *36*, 1720–1748.
39. Cioce, M., and Fazio, V.M. (2021). EphA2 and EGFR: Friends in Life, Partners in Crime. Can EphA2 Be a Predictive Biomarker of Response to Anti-EGFR Agents? Cancers *13*, 700.
40. Liang, L.-Y., Patel, O., Janes, P.W., Murphy, J.M., and Lucet, I.S. (2019). Eph receptor signalling: from catalytic to non-catalytic functions. Oncogene *38*, 6567–6584.
41. Boyd, A.W., Bartlett, P.F., and Lackmann, M. (2014). Therapeutic targeting of EPH receptors and their ligands. Nat. Rev. Drug Discov. *13*, 39–62.
42. Barquilla, A., and Pasquale, E.B. (2015). Eph Receptors and Ephrins: Therapeutic Opportunities. Annu. Rev. Pharmacol. Toxicol. *55*, 465–487.
43. Zhou, Y., Zhou, B., Pache, L., Chang, M., Khodabakhshi, A.H., Tanaseichuk, O., Benner, C., and Chanda, S.K. (2019). Metascape provides a biologist-oriented resource for the analysis of systems-level datasets. Nat. Commun. *10*, 1523.
44. Aguirre-Gamboa, R., Gomez-Rueda, H., Martínez-Ledesma, E., Martínez-Torteya, A.,

Chacolla-Huaringa, R., Rodriguez-Barrientos, A., Tamez-Peña, J.G., and Treviño, V. (2013). SurvExpress: an online biomarker validation tool and database for cancer gene expression data using survival analysis. PLoS One *8*, e74250.

45. Yang, W., Soares, J., Greninger, P., Edelman, E.J., Lightfoot, H., Forbes, S., Bindal, N., Beare, D., Smith, J.A., Thompson, I.R., et al. (2013). Genomics of Drug Sensitivity in Cancer (GDSC): a resource for therapeutic biomarker discovery in cancer cells. Nucleic Acids Res. *41*, D955–D961.
46. Ghandi, M., Huang, F.W., Jané-Valbuena, J., Kryukov, G.V., Lo, C.C., McDonald, E.R., Barretina, J., Gelfand, E.T., Bielski, C.M., Li, H., et al. (2019). Next-generation characterization of the Cancer Cell Line Encyclopedia. Nature *569*, 503–508.
47. Lenz, G., Wright, G., Dave, S.S., Xiao, W., Powell, J., Zhao, H., Xu, W., Tan, B., Goldschmidt, N., Iqbal, J., et al. (2008). Stromal gene signatures in large-B-cell lymphomas. N. Engl. J. Med. *359*, 2313–2323.
48. Leich, E., Salaverria, I., Bea, S., Zettl, A., Wright, G., Moreno, V., Gascoyne, R.D., Chan, W.-C., Braziel, R.M., Rimsza, L.M., et al. (2009). Follicular lymphomas with and without translocation t(14;18) differ in gene expression profiles and genetic alterations. Blood *114*, 826–834.
49. Zhan, F., Huang, Y., Colla, S., Stewart, J.P., Hanamura, I., Gupta, S., Epstein, J., Yaccoby, S., Sawyer, J., Burington, B., et al. (2006). The molecular classification of multiple myeloma. Blood *108*, 2020–2028.
50. Herold, T., Jurinovic, V., Metzeler, K.H., Boulesteix, A.-L., Bergmann, M., Seiler, T., Mulaw, M., Thoene, S., Dufour, A., Pasalic, Z., et al. (2011). An eight-gene expression signature for the prediction of survival and time to treatment in chronic lymphocytic leukemia. Leukemia *25*, 1639–1645.

STAR★METHODS

KEY RESOURCES TABLE

REAGENT or RESOURCE	SOURCE	IDENTIFIER
Antibodies		
Rabbit monoclonal anti-Phospho-Src (Tyr416) (clone D49G4)	Cell Signaling Technology	Cat#6943 RRID:AB_10013641
Mouse monoclonal anti-ACTB (clone ARC5115-01)	ABclonal	Cat#AC026 RRID:AB_2768234
Bacterial and virus strains		
MLS-Efnb1	Li et al.[24]	N/A
MLP-Stmn1	This paper	N/A
MLP-Stmn1-S28A	This paper	N/A
Chemicals, peptides, and recombinant proteins		
Dasatinib	Selleck	Cat#S1021
Ibrutinib	Selleck	Cat#S2680
MK-2206	Selleck	Cat#S1078
Cytarabine	Selleck	Cat#S1648
Methotrexate	Selleck	Cat#S1210
Gemcitabine	Selleck	Cat#S1714
Topotecan	Selleck	Cat#S1231
Doxorubicin	Selleck	Cat#S1208
Vincristine	Selleck	Cat#S1241
Cisplatin	Selleck	Cat#S1166
Oxaliplatin	Selleck	Cat#S1224
Decitabine	Selleck	Cat#S1200
Dimethyl sulfoxide	Merck	Cat#V900090
Dimethylformamide	Merck	Cat#D4551
Deposited data		
The mass spectrometry data of EV and Efnb1 cells	ProteomeXchange	PXD038838
Original western blot image	Figshare	https://doi.org/10.6084/m9.figshare.24442741
Experimental models: Cell lines		
Murine B-cell lymphoma cell line: Eμ-myc; Cdkn2a$^{-/-}$	Li et al.[24]	N/A
Recombinant DNA		
Retroviral vector: MLS and MLP	Li et al.[24]	N/A
cDNA for Efnb1	Li et al.[24]	N/A
cDNA for Stmn1	This paper	N/A
cDNA for Stmn1-S28A	This paper	N/A
Software and algorithms		
R x64 4.0.3		www.rstudio.com/
Metascape	Zhou et al.[43]	https://metascape.org/
SurvExpress	Aguirre-Gamboa et al.[44]	http://bioinformatica.mty.itesm.mx/SurvExpress
Other		
The Cancer Proteome Atlas (TCPA) database	Yang et al.[30]	https://tcpaportal.org/
Genomics of Drug Sensitivity in Cancer (GDSC) database	Ghandi et al.[45]	https://www.cancerrxgene.org/
Cancer Cell Line Encyclopedia (CCLE) database	Li et al.[46]	https://sites.broadinstitute.org/ccle/
Cell Model Passports	Wellcome Sanger Institute	https://cellmodelpassports.sanger.ac.uk/

RESOURCE AVAILABILITY

Lead contact

Further information and requests for resources and reagents should be directed to and will be fulfilled by the lead contact, Xiaoxi Li (lixiaoxi@ujs.edu.cn).

Materials availability

Requests for materials should be directed to the lead contact.

Data and code availability

- The mass spectrometry data have been deposited at the ProteomeXchange repository and are publicly available as of the date of publication. Accession numbers are listed in the key resources table. Original Western blot images have been deposited at Figshare and are publicly available from the date of publication. The DOI is listed in the key resources table.
- This paper does not report original code.
- Any additional information required to reanalyze the data reported in this paper is available from the lead contact upon request.

EXPERIMENTAL MODEL AND STUDY PARTICIPANT DETAILS

For cell lines

Murine B-cell lymphoma cell line *Eμ-myc;Cdkn2a*$^{-/-}$ was a kind gift from Prof. Hai Jiang at the Center for Excellence in Molecular Cell Science. *Eμ-myc;Cdkn2a*$^{-/-}$ cell line was cultured in 45%DMEM, 45%IMDM, 10% fetal bovine serum, supplemented with 100 U/ml penicillin and streptomycin, 25μM β-mercaptoethanol. The carefully regulated incubation environment maintained a consistent 5% CO2-saturated humidity and a stable temperature of 37°C to facilitate optimal cell growth and proliferation. *Eμ-myc;Cdkn2a*$^{-/-}$ cell line is derived from female mice according to RNA-seq data. PCR-based test for mycoplasma contamination was performed every two weeks.

METHOD DETAILS

Data acquisition and correspondence analysis

Drug IC50 dataset of drug panel and expression dataset of gene panel of DLBCL cell lines were downloaded from Genomics of Drug Sensitivity in Cancer (GDSC)[45] and Cancer Cell Line Encyclopedia (CCLE).[46] Annotation information for cell lines was downloaded from the Cell Model Passports.

Correspondence analysis of IC50 data and gene expression data was performed using the FactoMineR package in R Studio.

RPPA data analysis

Reverse phase protein array (RPPA) data of human DLBLC cell lines was downloaded from The Cancer Proteome Atlas (TCPA).[30] The normalized (level 4) protein expression values of 214 proteins/phosphoproteins were used for differential expression analysis. The significant difference of each comparison was analyzed by unpaired t-test and p values of <0.05 were considered significant.

Constructs

Gene of interest (GOI) with Kozak sequence GCCACC were amplified from cDNA of MA cells and cloned into retroviral vector MLS (LTR-MCS-SV40-GFP) or MLP (LTR-MCS-PGK-Puro-IRES-GFP). Efnb1 had been cloned into MLS in a previous study.[24] Stmn1 and Stmn1 S28A were amplified from cDNA and cloned into MLP in this study. MSCV retroviral vectors with a helper plasmid were co-transfected into HEK293T cells to produce retrovirus. GOI-GFP stable cell lines were established by retrovirus infection with polybrene (20 μg/ml). MLP-based stable cells (Stmn1 and Stmn1 S28A) were selected with puromycin (μug/ml). Fluorescence-activated cell sorting (FACS) was performed using FACSAria II (BD) to sort MLS-based stable cells (Efnb1). The single-clone cell strains were established through the dilution method, in which about 30 cells were seeded in 96 wells of a 96-well plate.

Chemicals

Dasatinib (S1021), Ibrutinib (S2680), MK-2206 (S1078), Cytarabine (Ara-C, S1648), Methotrexate (MTX, S1210), Gemcitabine (GEM, S1714), Topotecan (TPT, S1231), Doxorubicin (DOX, S1208), Vincristine (VCR, S1241), Cisplatin (CDDP, S1166), Oxaliplatin (OXA, S1224), Decitabine (DAC, S1200) were purchased from Selleck, USA.

All chemicals but CDDP and OXA were dissolved in dimethyl sulfoxide (DMSO, V900090, Merck, USA) to concentrations of 10mM and aliquoted and stored at −20°C. CDDP and OXA were dissolved in Dimethylformamide (DMF, D4551, Merck, USA) to concentrations of 10mM and aliquoted and stored at −80°C. Working concentrations for all chemicals were determined by lethal dose tests.

Drug response analysis

GFP competition assay was performed as previous.[26] Retrovirus infected cells with 30%–50% GFP proportion were used in the GFP competition assay. 4x104 cells in 100μL of BCM and 100μL 2x working solution diluted by BCM were mixed and incubated. 200μL and 400μL of fresh BCM were added at 24h and 48h. 100μL cell suspension were taken out to analyze the cell viability and GFP% of untreated and treated at 48h and 72h.

In the GFP competition assay, cell viability was mainly used to evaluate whether the drug concentration achieved the effective lethal dose (LD). Drug concentration achieving LD80 to LD90 at 48h was optimal for most drugs in GFP competition assay. The living cells, which were PI (propidium iodide) negative population, were gated to analyze the percentage of GFP in untreated and treated samples. GFP% of untreated and treated at 48h or 72h was used to calculate the Resistance Index (RI), which was used to evaluate the effect of genetic modification on therapeutic response of cells to tested drugs.

RI=(G1-G1*G2)/(G2-G1*G2). G1, GFP% in untreated. G2, GFP% in treated.

Gradient dose analysis was performed as follows. EV cells or sorted Efnb1 cells were mixed with 2-fold drug working solution and incubated as GFP competition assay. 200μL of fresh BCM were added at 24h. 100μL cell suspension were taken out to analyze the cell viability at 48h.

Western blot analysis

Protein was extracted by RIPA buffer containing protease and phosphatase inhibitors. Protein samples were equally loaded with 25 μg protein on 10% gels and separated at 120V. PVDF membranes with transferred proteins were blocked with 5% milk in TBST and immunoblotted with the following antibodies: Rabbit monoclonal anti-Phospho-Src (Tyr416) (#6943, Cell Signaling Technology, 1:1000, USA), Mouse monoclonal anti-ACTB (AC026, ABclonal, 1:100000, CN). Chemiluminescent was detected by Amersham Imager 600 (GE Life Sciences, USA).

Mass spectrometry data analysis

Cells were harvested by centrifugation and washed with cooled PBS three times. The precipitates were quick freezing at −80 and shipped to biotech company for mass spectrometry analysis with dry ice. Each sample was collected three times as three biological replicates.

The mass spectrometry analysis process was as follows. First, proteins were extracted and the concentrations of proteins were measured with BCA method. After trypsin enzymatic hydrolysis, the processed samples of replicates were combined and analyzed by LC-MS/MS to obtain raw files of the original mass spectrometry results. After MaxQuant (1.6.2.10) analysis, match the data and obtain the identification results.

Pathway enrichment analysis

Pathway enrichment analysis of DPs and DEPs was performed with Metascape.[43] Pathway enrichment analysis has been carried out with GO Biological Processes. All genes in the genome have been used as the enrichment background.

Prognostic analysis

Survival analysis was performed with the online tool SurvExpress.[44] The following datasets were used for survival analysis. DLBCL, Lenz-Staudt GSE10846,[47] number of patients = 414. FL, Leich-Staudt, GSE16131,[48] number of patients = 184. MM, Shaughnessy, GSE2658,[49] number of patients = 559. CLL, Herold Bohlander, GSE22762,[50] number of patients = 107. The prognostic index (PI) was calculated by the expression value and the Cox model to generate the risk groups. The optimization algorithm was applied in risk grouping. The SurvExpress program was performed according to the tutorial.

COO classification

The COO score was calculated based on the expression of 20 ABC/GCB subtype associated genes and assigned to ABC, GCB, and unclassified categories. 12 genes associated with ABC classification were SH3BP5, IRF4, PIM1, ENTPD1, BLNK, CCND2, ETV6, FUT8, BMF, IL16, PTPN1. 8 genes associated with GCB classification were ITPKB, MME, BCL6, MYBL1, DENND3, NEK6, LMO2, LRMP, SERPINA9.

The gene expression values were quantile normalized and log2 transformed, and then z-normalized across the genes. The average of the z-scores was calculated for each sample to compute the ABC/GCB scores. The COO score as a combined subtype score was then computed by taking the difference in the ABC score to the GCB score.

If the COO score was >0.25 and its GCB score was <0.75, the sample was classified as ABC; If the COO score was < −0.25 and its ABC score was <0.75, the sample was classified as GCB. The rest of the samples belonged to the unclassified group.

QUANTIFICATION AND STATISTICAL ANALYSIS

GraphPad Prism Version 9 software (GraphPad Software, USA) was used for graphing and statistical analysis. The unpaired t-test and the log rank test were used as indicated in the figure legends. Data are presented as mean ± SEM and p value < 0.05 was considered statistically significant. *p < 0.05, **p < 0.01, ***p < 0.001, ****p < 0.0001 and n.s. indicates not significant (p > 0.05).